Anaerobic digestion of palm oil, ethanol, and tequila production by products: Effects of alkaline hydrothermal pre-treatment on sugars release and biogas composition.

Master thesis submitted to Delft University of Technology in partial fulfillment of the requirements for the degree of

Master of Science in Environmental Engineering
Faculty of Civil Engineering and Geosciences
Department of Sanitary Engineering

by
Magnolia García Solano
Student number: 4749154

Assessment Committee:

Prof. Dr.ir. Jules van Lier
Dr.ir. Ralph Lindeboom
Dr. Ivan Buijnsters

Daily supervisor

Dr. Laís Américo Soares

Delft, June 2020

ABSTRACT.

This study explored the interactions between alkaline hydrothermal pretreatment (AHPT) operational conditions temperature (°C), NaOH concentration (M) and residence time (min) on the compositional characteristics of the solid (SH) and liquid hydrolysate (LH) obtained from AHPT of sugarcane bagasse (SCB), empty fruit bunch (EFB) and agave bagasse (AB). The experimental design was carried out with a three factors five levels ($-\alpha$, -1, 0, 1, and $+\alpha$) central composite rotatable design. Response variables for the liquid hydrolysate included glucose, xylose and arabinose content. Whereas the effects on the solid hydrolysate were evaluated with delignification and solids recovery (%). Biogas production and in situ biogas upgrading by co digestion of SH and NaOH rich LH was evaluated against mono digestion of raw and treated fibers. Therefore, methane production and methane content in the biogas were also considered response variables.

Compositional characteristics were fiber dependent. Glucose, xylose and arabinose were found in SCB and AB LHs whereas for EFB LH cellobiose was also detected. A significant (p-value <0.05) linear interaction between treatment temperature and glucose release was found for SCB and AB. EFB showed significant (p-value <0.05) a quadratic interaction between temperature and retention time with glucose release. Arabinose presented a significant (p-value <0.05) linear positive interaction with temperature and NaOH concentration in all fibers. Delignification of SCB had a significant (p-value <0.05) negative correlation with the coupled effect of temperature and NaOH concentration. Solids recovery showed a significant (p-value <0.05) negative interaction with temperature and NaOH concentration for all fibers.

Methane production from SCB hydrolysates co digestion presented significant (p-value <0.05) interaction with NaOH concentration and retention time. EFB hydrolysates co digestion presented a significant (p-value <0.05) interaction with temperature and NaOH concentration. Methane content in biogas presented a significant (p-value <0.05) linear interaction with temperature and NaOH concentration. No energy gain from pretreated SCB was observed. A maximum energy gain of 3.5MJ Kg^{-1} for pretreated empty fruit bunch. Agave bagasse presented a maximum net energy gain of 4.8 MJ Kg^{-1}.

Keywords: Empty fruit bunch; sugarcane bagasse; agave bagasse; hexoses; pentoses; lignin degradation.

Contents

Abbreviations list

AB	Agave bagasse
AD	Anaerobic digestion
AHPT	Alkaline hydrothermal pretreatment
BMP	Biomethane potential
CCRD	Central composite rotatable design
CP	Central point
CSP	Concentrated solar power
EFB	Empty fruit bunch
LB	Lignocellulosic biomass
LH	Liquid hydrolysate
RSM	Response surface methodology
SCB	Sugarcane bagasse
SH	Solid hydrolysate

List of figures

List of tables

Acknowledgements.

Thank you Dr.ir. Ralph Lindeboom for your constructive feedback, and patient guidance. Most of all thank you for your support, understanding and continuous encouragement in the past months.

Thank you Dr. Laís Soares for all the great experiences that we shared. For all the knowledge that you transmitted to me and the innumerable times that you helped me. I admire you not only as a researcher but also as a friend.

Thank you Prof. Dr.ir. Jules van Lier, and Dr. Ivan Buijnsters for their time, constructive feedback and understanding.

I wish to thank Magela Odriozola, Antonella Piaggio, Javier Pavez, Julia McGregor, Mohammed Jafar, Armand Middeldorp for the many times that you help me through the course of this project and all the knowledge that you shared with me.

Mamita, muchas gracias por haberme permitido soñar, por apoyarme en cada una de mis metas, por creer en mí, te amo. Rosita, Yiyi, Alte, Ninet (Nanis), los amo hermanitos gracias por todo las experiencias que hemos compartido y por estar cerca aun en la distancia. Teresa Rodríguez, Josué García, Joel Dupuy, Azucena García, Astrid García, gracias por todo el apoyo que me han brindado y por creer en mí siempre.

Diana Marquez, Julia Osorio, Yessica Hernández, Laura Rodríguez, Ariana Baizabal, Veronica Nostroza, Angélica Roa, Hugo Morales, Ana Cordova, Judith Lopez, Leo Figueroa, Jorge Romero, Daniel Castillo, Berenice García, Aldo Trejo, Lucero Herrera, Gerardo Martínez, Ilse Cabrera, Adriana Urquiza, Karla Arteaga, Daniel Toscano, Grettel, Aviles, Martha Sosa, Juan Hernández, Anahí Hernández, I am grateful for having you in my life. Thank you for the innumerable times that you have been there to support me, for helping me fight my fears and pursue my dreams. For believing in me.

Eng. Jose Luis Cuevas, Eng. Jose Antonio Gonzalez, Dr. Eliseo Hernández, Dr. Epifanio Marín, thank you for all the lessons, for challenging me to go out of my comfort zone, for supporting my dreams. I admire you so much.

Adrian Gonzalez, Victor García, Viridiana Moreno, Daniël Huisman, David Arellano, Renita Daranianti, Shreyasi Hait, Weizhao Li, Kevin Septian, Sahibzada Hamza, Isis Zazueta, Felipe Orozco, Bertalan Varga, Ashwini Petchiapan, Shreya Trikannad, Mrinal Roy, Apoorva Seeram, Sasidhar KB, Rubayat Sobhan, Daniel Dacomba, Jingdan Lou, Kayleigh Lieverse, Rita Bader. Thank you for all the times you lift my spirit, for your understanding, kindness and friendship.

Dr. Dulce Miranda, Dr. Paula Meesters, Dr. Jimena Gomez for your help through the rough times.

1. INTRODUCTION.

Currently, the global energy mix relies on fossil fuels (*e.g.*, petroleum, natural gas, and coal). According to the International Energy Agency (2017), global energy demand is expected to increase by about 27% from 2017 to 2040; the higher energy demand could pose a challenge to energy security. In order to cope with the demands of power, heat, and transport in a sustainable manner; this is, avoiding acute effects on the environment, renewable energies share in the global energy mix must be increased (IRENA, 2018; Mao *et al.*, 2015).

Bioenergy resources such as municipal solids wastes, sewage, industrial wastewater, livestock dung, forestry resources, agricultural resources, and manufacturing processes byproducts are among the main renewable resources. Bioenergy production from agro - based industrial byproducts such as lignocellulosic biomass (LB) has been gaining importance in recent years as they do not represent a threat to food security nor to soil fertility. LB is largely produced in developing countries, reaching a global production of 60 billion tons (Carrillo-Nieves *et al.*, 2019). For instance, sugarcane bagasse (SCB) is one of the main residues produced in the Brazilian sugar and alcohol industry, which reaches around 200 million tons per year (Santos *et al.*, 2016). In the same way, Malaysia and Indonesia are among the largest producers of palm oil accounting for 80-85% of the global capacity (Zahan & Kano, 2018). Several by-products such as empty fruit bunch (EFB) are generated in the production of palm oil; EFB waste reaches up to 6.5 ton/ha/year, and it is the most abundant accounting for 23% of the initial fresh fruit bunch (O-Thong *et al.*, 2012). Similarly, in Mexico tequila production involved the generation of 377,000 tons of a waste solid fraction know as agave bagasse (AB), only in 2016 (CRT, 2016; Palomo *et al.*, 2018).

LB is composed, in majority, of cellulose, hemicellulose, and lignin. This complex structure presents recalcitrant characteristics that decrease bioenergy generation processes efficiency (Fan *et al.*, 2016: Mustafa *et al.*, 2018). Lignin and hemicellulose block away any enzymatic activity on the cellulose due to the structure and distribution of lignin; coupled to this, cellulose crystalline regions are resistant to acid, alkaline or enzymatic hydrolysis (Song *et al.*, 2005; Taherzadeh & Karimi, 2007). Therefore, a pre-treatment that disrupts the lignin-hemicellulose-cellulose matrix is needed to enhance the LB biodegradability rate.

The pre-treatment processes are generally classified as physical, chemical, thermal, and biological. Among the chemical pre-treatments, we can find the alkaline hydrothermal pretreatment (AHPT) which enhances enzymes' accessibility to the cellulose by disrupting the bond between lignin and hemicellulose promoting lignin solubilisation (Chang & Holtzapple, 2000; Sun *et al.*, 2004). A range of alkalis (*e.g.*, $Ca(OH)_2$, KOH, Na_2CO_3, and NaOH) effect on LB biomethane potential (BMP) has been studied. Of these NaOH has repeatedly been found to have higher yields due to its higher lignin degradation rate and higher fiber swelling capacity that increase the accessibility of microorganisms to cellulose (Nunes *et al.*, 2020; Phitsuwan *et al.*, 2016; Shah *et al.*, 2018).

AHPTs can be carried out at different operational conditions, such as alkali concentration, temperature, retention time, among others. The pretreatment yields a solid hydrolysate (SH) composed of cellulose and lignin (in its majority) and a liquid hydrolysate (LH) on which hemicellulose and cellulose degradation products can be found. At mild operational conditions, cellulose is degraded into glucose whereas hemicellulose is degraded into a range of sugars such as xylose, mannose, galactose, along with glucose. If the conditions are more severe, the sugars will be further degraded into anaerobic digestion inhibitory compounds (*e.g.*, 5- hydroxymethylfurfural (5-HMF), furfural, and levulinic acid). Conclusions of a range of studies (Arreola *et al.*, 2015; Rios *et al.*, 2017; Simanungkalit *et al.*, 2017) suggest that the hydrolysates composition varies according to the operational conditions settings consequently, changes in hydrolysates composition lead to different bioenergy production yields.

Biogas is produced through anaerobic digestion (AD) which consists of a sequence of reactions in the absence of oxygen. Anaerobic digestion processes can be carried out at a wide range of temperatures; the most common being 35°C and 55°C which are identified as mesophilic and thermophilic range, respectively. Conventionally, only the SH serve as feedstock for the anaerobic digestion processes. However, the co-digestion of the SH and LH has some advantages. For instance, in situ biogas upgrading by solubilisation of CO_2 on the alkaline digestate as well as reduced environmental impacts. Additionally, a higher exploitation of the raw material is achieved reducing environmental impacts since no polluting streams are discarded.

Evaluating the interactions of the AHPT operational conditions with the hydrolysates composition and their bioenergy potential can be achieved by employing central composite rotatable design (CCRD) and response surface methodology (RSM). The decision on the most viable AHPT operational conditions must consider the net energy gain in terms of raw dry fiber used. Energy requirements for NaOH production as well as energy needed for maintaining the hydrothermal process decrease the net energy gain. Some studies have explored the implementation of concentrated solar power in lignocellulosic biomass hydrothermal pretreatment; further application of this technology for NaOH thermal recovery could contribute to an increase in the net energy gain.

In this work, the effects of AHPT on sugars recovery biogas yield and composition from SCB, EFB, and AB were studied. To this end, two main experiments were performed for these fibers. First, AHPT was carried out varying temperature, retention time, and NaOH concentrations. The variations in the conditions were set by CCRD. After this, manometric BMP tests were conducted to test the effects of the different pretreatment conditions on the fiber's biodegradability. BMP tests were carried out with both co-digestion and mono-digestion of the SH and LH to test the effects of NaOH on the biogas production and composition. Subsequently, RSM was applied to determine the interactions between the operational conditions with the response variables (*i.e.*, sugars recovery, BMP, and biogas composition). Lastly, the calculation of the net energy gain from AHPT and the theoretical evaluation of the application of a concentrated solar power system (CSP) for NaOH thermal recovery from the AD digestate were estimated.

2. LITERATURE REVIEW

2.1. Energy and Environment

Throughout time, global energy demand has shown an increasing tendency. Development has brought not only more opportunities but also more challenges to policymakers, governments, and the population in general. In the past years, the effects of worldwide unsustainable practices have started to manifest which have led to the creation of climate change mitigation international agreements. For instance, the Paris agreement and the Sustainable Development Goals which consider the reduction in the emission of greenhouse gases as one of the main means to mitigate climate change. Currently, the energy mix is dominated by fossil fuels; energy production from these sources accounts for more than 50% of the total greenhouse gasses emissions (IPCC, 2014). Several reports (BP, 2019; IEA, 2019; IRENA, 2018; Shell, 2011) show the relationship between different climate change scenarios and the energy mix. A higher renewable energies share in the global energy mix has been considered as a viable strategy to cope with the increase in energy demand in a sustainable manner. For instance, Gielen *et al.*, 2019 estimated that the renewable energy share in the total global energy mix must be increased from the current 19% to 65% by the year 2050 in order to achieve the energy transition. Additionally, these studies suggest that coupling renewables energies production along with an increase in energy efficiency would allow a higher reduction in the emission of greenhouse gases.

Emerging economies will increase their energy demand in the coming years as development brings along an increase in energy use for electrification and transportation purposes. Developing countries will not only be the main contributors to the increase in energy demand in the coming years; they will also be responsible for the generation of large quantities of agro-industrial residues.

2.2 Lignocellulosic biomass (LB)

The production of sugar, palm oil and tequila is and will continue to be among the main contributors to the gross domestic product (GDP) in Brazil, Malaysia and Mexico, respectively (Caldarelli *et al.*, 2017; Sánchez *et al.*, 2020; Sadhukhan *et al.*, 2018). As the demand for these products raises so does the environmental impacts created due to improper disposal of the byproducts generated. Traditionally, SCB was employed to make the sugar and ethanol industries self-sufficient in terms of energy use. However, the introduction of high-pressure boilers allowed an increase in the energy efficiency of cogeneration plants, therefore, the SCB feed requirements decreased leading to a surplus of bagasse (Savou *et al.,* 2019). Current EFB disposal practices involve conversion into pellets for co-firing applications, discarding it into landfills as well as its use as organic mulch or fertilizer in plantations (Lam *et al.,* 2019). EFB contributes to an improvement in the nutrient level and vegetative growth in soils with reduced fertility. There are, however, some drawbacks to these practices: the pests in the fields as well as soil and water pollution by oxidation of the compounds present in EFB. AB is mainly used as compost (70%) and to a lesser extent, it can be used in the manufacturing of bricks, furniture, and packaging materials. However, a significant amount is disposed of without treatment which generates environmental damage and nuisance due to the diffusion of leachates into the soil and unpleasant smells (González *et al.,* 2018; Sánchez *et al.,* 2020).

There is an opportunity to make use of LB as a reliable feedstock on sustainable energy generation. Ullah *et al.*, (2015) found that LB has the potential to cover most of the global energy demand projected by the International Energy Agency for the year 2030. Nanda *et al.,* (2015) stated that the production of liquid and gaseous biofuels from LB offers several advantages over conventional energy sources, such as energy security, development of the rural economy. In addition, since LB amount being wrongly disposed could decrease, greenhouse gases emissions could be reduced contributing to climate change mitigation. Energy production from agro-industrial residues can be considered carbon neutral under the assumption that the CO_2 released on the combustion of biomass is then consumed when biomass regrows (Woo *et al.*, 2019). Additionally, competition with food crops is avoided.

Agro-industrial residues contain a high amount of fermentable sugars; the main components of the LB are cellulose, hemicellulose, lignin, extractives/volatiles, and ash (Carrillo-Nieves *et al.,* 2019; He *et al.,* 2015; Williams *et al.*, 2017). Cellulose and hemicellulose are chain polysaccharides; lignin is a phenyl-propane polymer. LB components are strongly interlinked by covalent and non-covalent bonds forming the lignocellulosic matrix. Cellulose is a polysaccharide of glucose monomers joined by glycosidic linkages; the polysaccharide structure leads to a high presence of hydroxyl groups along the cellulose backbone that forms highly arranged hydrogen bond networks that give cellulose a crystalline structure (Sun *et al.,* 2016). On the other hand, the hemicellulose structure can be considered as amorphous and more susceptible to hydrolysis (Williams *et al.,* 2017). Xylose, mannose, and glucose are among the main carbohydrates that form the hemicellulose units. Lignin is a phenolic polymer that does not contain carbohydrates; it gives the structural strength to the lignocellulosic materials (Williams *et al.*, 2017). LB cannot be directly used in bioenergy production as its complex structure hinders its full exploitation as a substrate. Cellulose crystallinity provides a robust structure that cannot be broken down easily whereas lignin content cause hydrophobicity of the LB resulting in a decrease in biodegradation (Costa *et al.*, 2014). In the same manner, volatiles content in the biomass such as acetic acid and furans can negatively affect the efficiency of biological conversion processes such as AD. Therefore, changes in the structural and compositional characteristics of the biomass need to be performed aiming for higher bioenergy yield.

LB compositional properties are fiber dependent; the variations are mainly attributed to the variations in the production, harvesting, collection and storage practices that are applied to the fibers; parameters such as moisture and ash content, carbohydrates distribution and heating values vary from fiber to fiber (González *et al.*, 2019; Williams *et al.*, 2017). Table 1 shows a general overview of the variations in the compositional characteristics of SCB, EFB, and AB. The differences in the fibers´ composition, especially on lignin content, lead to diverse bioenergy yields (He *et al.*, 2015; Tsapekos *et al.*, 2018).

Table 1 Compositional fractionation (%) of empty fruit bunch (EFB), sugarcane bagasse (SCB) and agave bagasse (AB)

Fiber	Hemicellulose	Cellulose	Lignin	Ash	Reference
SCB	27.6	42.2	21.56	2.84	de Moraes *et al.*, 2015
EFB	12.07	59.14	25.33	1.16	Zianor *et al.*, 2017
AB	13.95	54.6	16.2	4.5	Robles *et al.*, 2018

2.3 Pretreatment

There are several energy production processes that use LB as feedstock such as bioethanol, bio hydrogen, biodiesel, biogas, among others (Patel *et al.*, 2016; Phuttaro *et al.*, 2019; Vieira *et al.*, 2020; Wang *et al.*, 2019). It has been estimated that biomethane could supply at least 70% of the current natural gas consumption (Woo et al 2019). Biogas can be used in power generation or as an alternative to natural gas. Sadhukhan *et al.*, (2018) reported that biogas with a methane content above 96% can save 0.0793 CO2 equivalent / MJ or 0.12 CO2 equivalent / MJ when injected into the natural gas grid or when used in CHP systems respectively. However, in order to make bioenergy production from LB feasible, it is necessary to tackle one of its main constrains, its recalcitrant properties. The enzymatic attack on lignocellulosic materials in fermentation processes is limited by the three-dimensional structure of lignin. When LB is biodegraded in bioenergy production systems such as AD, the hydrolysis of the biomass is the first rate-limiting step. Buffiere *et al.*, (2006) found that a lower biodegradability of different waste streams is positively related to the lignin and hemicellulose content.

LB pretreatments include: physical (*e.g.*, sieve-based grindings, jet milling, ultrasonic, microwave irradiation), chemical (*e.g.*, alkaline, acid, organoslov, ionic), thermal (*e.g.*, hydrothermal pretreatment, steam explosion), and biological (*e.g.*, fungal, enzymatic). Coupling of chemical and thermal pretreatment for instance, AHPT has repeatedly shown higher impacts on the biogas yield of a range of agro-industrial residues (Mancini *et al.*, 2016). The main objective of LB pretreatment prior to anaerobic digestion processes is the exposition of the cellulose by solubilisation and removal of hemicellulose and lignin, respectively. AHPT disrupts the ester linkages that are found between xylan and lignin resulting in a higher porosity of the fibers and higher surface accessibility. Swelling of the fibers occurs due to solvation and saponification reactions leading to lignin solubilisation, hemicellulose removal, disruption of interlinking ester bonds among others. With this, anaerobic microorganisms are more capable of accessing the substrates, which leads to higher biogas yields (Mancini *et al.*, 2016; Mao *et al.*, 2015).

AHPT will lead to structural, morphological, and compositional changes in the biomass; the effects will vary according to the variations in the operational conditions. Cellulose and hemicellulose are degraded into more readily available substances such as sugars, which contributes to an increase in the biogas yield (Mancini *et al.*, 2016). The first step in LB AHPT is the liberation of hemicellulose since it is more susceptible to thermal decomposition. This difference is attributed to the lower molecular weight and shorter lateral chains of hemicellulose in comparison to those of cellulose (Sadhukhan *et al.*, 2018**)**. Hemicellulose solubilisation has been found to start at temperatures as low as 150°C, it is followed by lignin degradation at 180°C. Glucose is released from cellulose due to the breakage of the β-(1-4)-glycosidic linkages. Figure 1 shows the different degradation products from LB. The hydrolysis of cellulose yields different degradation products according to the treatment severity; at low severity glucose units are released; at mild severity 5-hydroxymethyl-2-furaldehyde (HMF) is formed; if the severity increases further degradation into formic and levulinic acid can be observed (He *et al.*, 2015). Hemicellulose is mainly degraded to mono and oligosaccharides such as xylose, arabinose and glucose. However, if the pretreatment is carried out at high severity the formation of inhibitory compounds (*e.g.*, furfural and 5-HMF) might occur (He *et al.*, 2015).

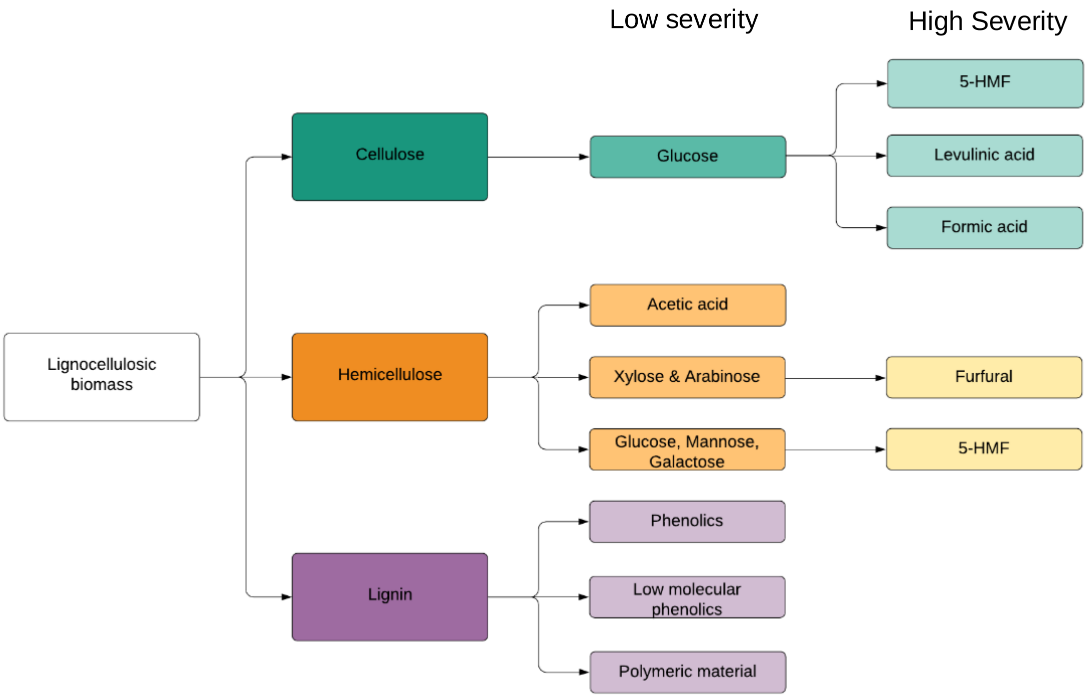

Figure 1 Lignocellulosic biomass degradation products

AHPT effects on biomass recalcitrance depend temperature, alkali concentration, and retention time. For instance, AHPT carried out at low temperatures contribute to the swelling of the lignocellulosic fibers. NaOH effect on cellulose range from swelling to full solubilization at low and high concentrations, respectively (Mancini *et al.*, 2016). At high temperature breakdown of lignin and hemicellulose into soluble fractions occurs, therefore, more cellulose is accessible to the microorganisms (Mao *et al.*, 2015). The operational conditions for AHPT are related with the NaOH concentration of the solution in which the biomass is dissolved. According to Mirahmadi *et al.*, (2010) low NaOH concentrations (0.5-0.4%), high temperature, and pressure are needed to achieve the disintegration of hemicellulose and lignin. On the other hand, if high concentrations are added to the system (6-20%), relatively low pressure and temperature are needed for the dissolution and regeneration of cellulose. Egal *et al.,* (2007) adjudicate this to the dissolution capacity of NaOH in water. If the NaOH concentration is low, the hydrates are too large to be able to enter the cellulose fibers. At high NaOH concentrations (20%) the hydrates will be smaller in size which allows them to enter into the fibers and form crystals with the cellulose chains.

At high temperatures, the ester linkages that unify cellulose, hemicellulose, and lignin are broken down which results in degradation into sugars and formation of alkali stable end groups (Karimi *et al.,* 2013). The removal of hemicellulose is related to the temperature of the pretreatment; at high temperatures, higher degradation of hemicellulose, as well as re-deposition of lignin on the fiber surface due to cooling can be observed. He *et al.,* (2015) found that the biodegradability of the biomass does not depend on temperature alone but rather on the coupling of temperature and retention time, this is referred to as treatment severity. LB pretreatment needs to aim for integrity (maximum recovery of the sugars) of cellulose as it is the main substrate to be converted to biogas.

Conventionally, bioenergy processes make use of either the liquid or the solid lignocellulosic biomass hydrolysates due to sensitivity to lignocellulosic biomass degradation compounds. AD has been considered as a promising technique for the use of the liquid hydrolysates since microbial communities are capable of consuming hexoses (glucose, mannose, and galactose) and pentoses (xylose and arabinose). Biogas applications include its use in power generation, combined heat and power plants, its natural injection into the natural gas grid and use as transportation fuel. These application require different biogas qualities in terms of CO_2 content. Since AD is able to make use of lignocellulosic biomass degradation products, in situ biogas upgrading by means of SH and LH co digestion can be explored. An increase in methane content could be associated to the interactions between NaOH and the carbonate species present in the system.

2.4 Anaerobic Digestion (AD).

AD can be divided into 4 general stages. First, the hydrolysis of complex organic polymers, which are broken down into monomers such as sugar and organic acids, is carried out via enzymatic decomposition. In the second stage, acidogenesis, organic acids are converted into hydrogen, acetic acid, and intermediates such as propionic acid, butyric acid, among others. Acidogenesis intermediates are converted to acetic acid and hydrogen in the acetogenesis stage to be finally biodegraded in methane gas in the methanogenesis stage (Bajpai, 2017).

2.5 Central composite design (CCRD) and response surface methodology (RSM)

Testing the different interactions of AHPT operational conditions of the responses of interest is a time and resources demanding task. There are several conventional techniques used in experimental design; the main aim of these is to reduce the number of experiments thus decreasing the number of raw materials and reagents employed in the research whilst still getting reliable data. Commonly a one factor at a time is used which results in high experimental costs. CCRD coupled with RSM has been employed in the optimization of different processes along with the various knowledge disciplines (Li *et al.*, 2016; Lopes *et al.*, 2019; Prakash *et al.*, 2016; Senthivelan *et al.*, 2019).

2.6 Net energy gain

Bioenergy production in terms of raw dry fiber varies according to the treatment conditions since the amount of total volatile solids recovery and the methane production will vary along treatment conditions. Net energy gain can be defined as the extra energy gained in the AD of treated fibers in comparison to raw fibers minus the energy expenditure in the treatment stage. AHPT is a high energy consumption processes if one takes in consideration the amount of energy spent in NaOH production as well as the energy needed to maintain the hydrothermal reactor at the different pretreatment conditions. Therefore, alternative routes for AHPT reactor heating coupled with NaOH recovery would increase the net energy gain from AHPT processes contributing to an increased feasibility for application.

SCB, EFB and AB are produced at large quantities in Brazil, Malaysia and Mexico, respectively. Coincidentally, these countries have high solar radiation ranging from 4.5 to 6 KWh m^{-2}. Solar energy, more specifically, concentrated solar power has been used in bioenergy productions systems as an alternative energy saving strategy (McGregor, 2019; Xiao *et al.*, 2019). The energy needed for NaOH thermal recovery from AD digestate could be provided with CSP.

3. RESEARCH QUESTIONS AND HYPOTHESIS

3.1. Problem statement.

LB recalcitrant properties hinder its application as feedstock for bioenergy productions processes. AHPT contributes to the disruption on the fibers main components (*i.e.*, lignin-cellulose-hemicellulose); the changes depend on the AHPT operational conditions set points and are fiber specific. Biogas yield depends on the SH and LH composition. Therefore, evaluation of the interactions between the operational conditions with hydrolysates compositions and biogas yield needs to be evaluated and optimized for the fibers of interest. In this study SCB, EFB and AB were evaluated.

3.2 Main Research Question

What is the effect of AHPT on lignocellulosic biomass in terms of sugars release and biomethane production?

3.3. Specific research questions and hypothesis

- What is the effect of AHPT on LB recalcitrant characteristics and sugars availability?

  Sugars concentration and composition in the SH and LH will be fiber and AHPT conditions specific. At mild conditions, pentoses and hexoses will be the main degradation products in the LH whereas cellulose exposure will be increased in the SH due to delignification and hemicellulose solubilization. At high treatment severities, pentoses and hexoses will be further degraded into inhibitory compounds.

- What is the effect of AHPT on LB biogas yield and biogas composition through thermophilic AD?

  Biogas yield will be fiber and AHPT conditions specific. At mild conditions, enhanced biogas yield will be observed due to higher cellulose exposure. At high treatment conditions biogas yield will decrease due to inhibitory compounds presence in the hydrolysate and/or re condensation of lignin in the SH.

- Does co-digestion of SH and LH from AHPT of LB contribute to in-situ biogas upgrading through CO_2 solubilisation? If so, to what extent?

  Co digestion will increase methane content in the biogas by interactions between carbonate species and NaOH present in the LH.

- Does NaOH regeneration contribute to energy savings in the AHPT of LB?

  The use of a concentrated solar power system for thermal recovery of NaOH would decrease the energy consumption of LB AHPT processes.

3.4. Main objective.

To determine what is the efficiency of AHPT on LB in terms of sugars release and Biomethane production.

3.5 Specific research objectives.

- To identify, qualitatively and quantitatively, the effect of AHPT on the recalcitrant properties of LB and sugars recovery.
- To assess the impact of AHPT on LB biodegradability in thermophilic batch AD.
- To determine to what extent co-digestion of SH and LH from AHPT of LB contributes to in-situ biogas upgrading by means of CO_2 solubilisation.
- To discuss and theoretically analyze the potential energy savings from thermal NaOH regeneration from the digestate.

4. MATERIALS AND METHODS.

4.1. Substrates, inoculum, and nutrients for alkaline hydrothermal pretreatment (AHPT) and biomethane potential (BMP) tests.

4.1.1 Raw lignocellulosic material sampling and reprocessing.

EFB fibers used for this study were obtained from SzeTech Engineering Sdn. Bhd., Selangor, Malaysia. SCB fibers were obtained from Laboratório Nacional de Biorrenováveis (lnbr), Campinas, São Paulo, Brazil. AB fibers were obtained from Casa Cuervo, Tequila, Jalisco, Mexico. All fibers were dried until a humidity lower than 10% was reached to be later stored in vacuum sealed plastic bags at 4°C. Prior to their use in characterization analysis and experimental tests, the fibers were milled to reach 1mm and 1-2cm of size, respectively.

4.1.2 Inoculum

The inoculum for this study was obtained from Wabico B.V., Waalwijk, Netherlands. In this plant, biogas is produced using residues from nearby plants (*e.g.*, egg factories and slaughterhouses) as substrate. The reactor operates in the thermophilic range at a semi-continuous mode with 10-15 min of feeding and 45-50 min digestion and a sludge retention time (SRT) of 60 days. Before the experimental test, the sludge was sieved through a 1mm mesh aluminum screen to be later incubated in an Innova® 44 incubator during one week. Alkalinity, pH, conductivity, volatile fatty acids, ammonia, total and soluble chemical oxygen demand, total and total volatile solids content of the inoculum were measured before and after BMP tests.

4.1.3. Nutrients solutions for biomethane potential (BMP) tests.

BMP tests require the addition of macro (15ml L^{-1} medium) and micro (7.5ml L^{-1} medium) nutrients solutions to guarantee optimum conditions for the microorganisms. Table 2 shows the characteristics of the solutions used. The solutions were stored at 4°C prior to use.

Table 2 Composition of nutrients solutions used for biomethane potential tests.

	Compound	**Concentration**
Macronutrients	NH_4Cl	170 g L^{-1}
	$CaCl_2$ 2 H_2O	8 g L^{-1}
	$MgSO_4$ 7 H_2O	9 g L^{-1}

Micronutrients	$FeCl_3$ 4 H_2O	2 g L^{-1}
	$CoCl_2$ 6 H_2O	2 g L^{-1}
	$MnCl_2$ 4 H_2O	0.5 g L^{-1}
	$CuCl_2$ 2 H_2O	30 mg L^{-1}
	$ZnCl_2$	50 mg L^{-1}
	HBO_3	50 mg L^{-1}
	$(NH_4)6Mo_7O_2$ 4 H_2O	90 mg L^{-1}
	Na_2SeO_3 5 H_2O	100 mg L^{-1}
	$NiCL_2$ 6 H_2O	50 mg L^{-1}
	EDTA	1 g L^{-1}
	HCl 36%	1 mL L^{-1}
	Resazurine	0.5 g L^{-1}
	Yeast extract	2 g L^{-1}

4.2 Alkaline hydrothermal pretreatment (AHPT)

4.2.1 Experimental design: Central composite rotatable design (CCRD) coupled with response surface methodology (RSM).

CCRD makes use of factors, this is, the operational variables that influence the performance of the process under study. CCRD use factorial and axial points that allow for the optimization of the interactions of the defined factors. The experiments are carried out randomly with central point (CP) that help to estimate the experimental error. CCRD coupled with RSM help to optimize a process by observing the single and coupled effect of the operational conditions on the response variables that are of importance to said process. The factors can present different interactions such as linear and quadratic. By means of process optimization, the quadratic interaction is preferred as it allows for the identification of an optimal point under the range studied. Figure 2 shows the factorial, axial, and CP distribution for a three-factor central composite rotatable design. An alpha (α) value of 1.682 is used in this design.

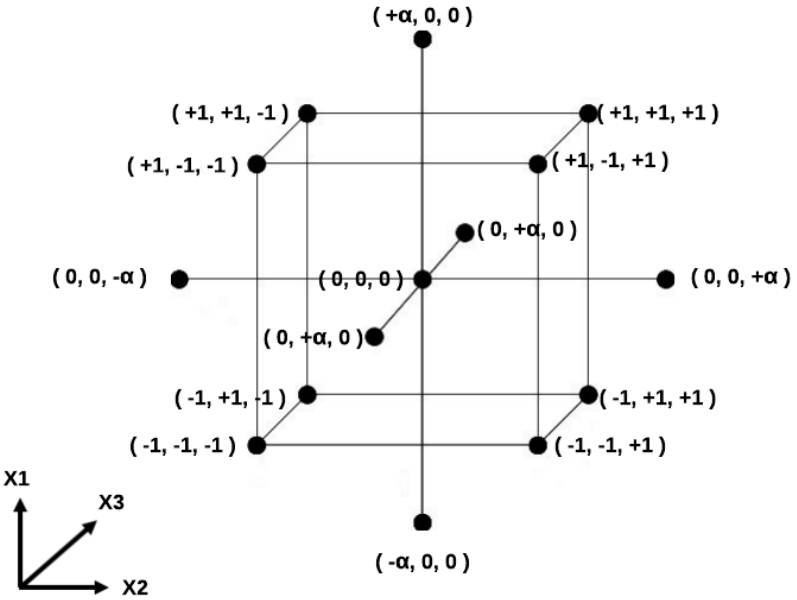

Figure 2 Central composite rotatable design (CCRD) for three factors with alpha (α) value of 1.682 adapted from Noman et al., 2018

To evaluate the individual and interactive effects of temperature, [NaOH] and retention time on the recalcitrant properties of lignocellulosic biomass (*e.g.*,, EFB and SCB) central composite rotatable design CCRD) and response surface methodology (RSM) were applied. To this end, Protimiza software (https://experimental-design.protimiza.com.br/e/5743163381645312) was used. The decoded values for each condition are mentioned in Table 3 The values were selected according to the influence that these three conditions have shown in the recalcitrant properties in previous studies for EFB, SCB and, AB. An alpha value of 1.682 was used to determine the axial points. Table 4 shows the levels and values for the 14 different conditions tested along with the CP. The conditions run in triplicates.

Table 3 Decoded values (*i.e.*, minimum, central, and maximum) for the operating conditions (temperature, [NaOH] and retention time) of alkaline hydrothermal pretreatment evaluated by central composite design with Protimiza software.

	Minimum (-1)	**Central (0)**	**Maximum (+1)**
Temperature (°C)	160	180	200
[NaOH]	1M	1.5M	2M
Retention time (min)	10	20	30

Table 4 Matrix of alkaline hydrothermal conditions and central point (CP) generated by STATISTICA software using central composite rotatable design.

Conditions	Factors (independent variables)					
	Temperature (°C)		[NaOH] (M)		Retention time (min)	
	Level	**Value**	**Level**	**Value**	**Level**	**Value**
1	(-1)	160	(-1)	1.00	(-1)	10
2	(-1)	160	(-1)	1.00	(+1)	30
3	(-1)	160	(+1)	2.00	(-1)	10
4	(-1)	160	(+1)	2.00	(+1)	30
5	(0)	180	(-α)	0.66	(0)	20
6	(0)	180	(0)	1.50	(-α)	3
7	(0)	180	(0)	1.50	(+α)	37
8	(0)	180	(+α)	2.34	(0)	20
9	(+1)	200	(-1)	1.00	(-1)	10
1	(+1)	200	(-1)	1.00	(+1)	30
11	(+1)	200	(+1)	2.00	(-1)	10
12	(+1)	200	(+1)	2.00	(+1)	30
13	(-α)	146	(0)	1.50	(0)	20
14	(+α)	214	(0)	1.50	(0)	20
CP	(0)	180	(0)	1.50	(0)	20

4.2.2 Reactor set up.

AHPT was carried out in a Parr pressure reactor (Figure 3). The temperature was controlled with a 4838 Parr reactor controller. The reactor chamber was filled with ±300ml of distilled water to account for evaporation losses. The biomass sample mixed with the NaOH solution was placed in a closed vessel that was then carefully placed in the reactor chamber. Both, the closed vessel and the reactor were flushed with inert gas (Nitrogen) during 1min. The solid to liquid ratio was fixed at 10% (w/w) with 10g of EFB fibers mixed with 100g of NaOH solution of the desired concentration. Once the sample reached the selected operational temperature, the selected retention time began.

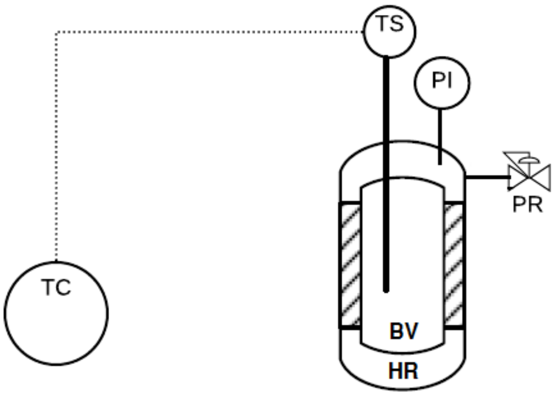

Figure 3 Hydrothermal reactor (HT) set up with biomass vessel (BV); temperature controller (TC); temperature sensor (TS); pressure indicator (PI) and pressure release valve (PR)

After reaching the desired retention time, the reactor was depressurized, and the sample was cooled down until room temperature. The pH values of the alkaline sample before and after pretreatment were measured. After pretreatment, the solid fraction was separated from the liquid by filtration of the sample through a Whatman sterile filters with a pore size of 0.45µm. The fibers were then washed with distilled water until neutral pH of the washing waste was reached; after this, the fibers were oven-dried for 24hrs at 105°C.

SH and LH, from each CCRD set of AHPT conditions, were analyzed to determine the effect of the severity of the LB structure. The selected response for the CCRD was the sugars (cellobiose, glucose, xylose, and arabinose) released.

4.3 Manometric biomethane potential (BMP).

Effects of AHPT on the bioenergy potential of SCB, EFB and AB was evaluated by means of manometric BMP tests. The BMP tests were carried out in 125ml Wheaton glass serum bottles placed on an Innova® 44 incubator operating under thermophilic (55 ± 0.5 C) conditions with gentle stirring (55 rpm). Blank and positive controls were carried out along with the different conditions. Figure 4 shows the conditions tested for SCB, EFB, and AB. Mono digestion of the liquid and solid hydrolysates was carried out for the CP conditions of the AHPT. Co digestion was evaluated for all 14 conditions of the CCRD along with the CP. The hydrolysates BMP on mono digestion and co digestion systems was compared to that of the raw fiber. All reactors were fed with the same amount of inoculum (*i.e.*, 45ml) in a volatile solids ratio of 2:1 with respect to the substrates. The pH of the reactors was adjusted to 7 ± 0.2 using 1M HCl or 1M NaOH, accordingly. After this, each reactor was sealed with aluminum caps and rubber stoppers. The reactors were flushed with N_2/CO_2 in a mixture of 80% to 20% prior to incubation. The biogas produced was accumulated in the headspace. The headspace pressure and biogas composition were measured weekly to estimate the methane production. Total and total volatile solids, total and soluble chemical oxygen demand, volatile fatty acids, ammonia, pH, alkalinity, and conductivity of all reactor contents were measured right before and after incubation.

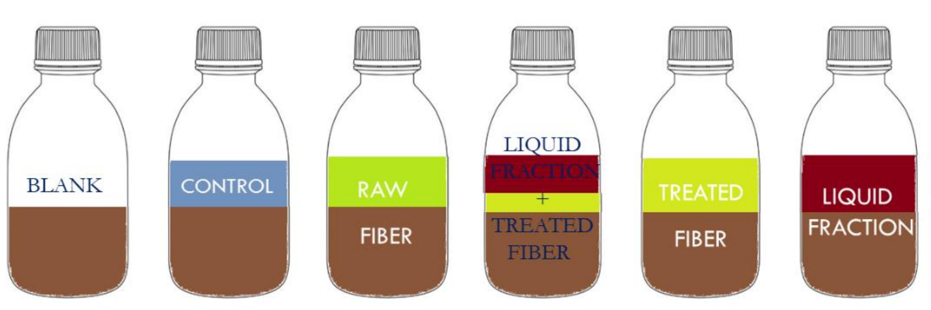

Figure 4 Manometric biomethane potential conditions tested for sugarcane bagasse, empty fruit bunch and agave bagasse

4.4 Net energy gain.

The estimation of the energy required for maintaining the AHPT was estimated following Paul & Dutta (2018).

$$Etotal = E_B + E_W \qquad \text{Equation 1}$$

Where E_B is the energy required to heat the biomass mixture (KJ) and E_W is the energy required to heat the dilute alkali solution (KJ).

$$E_B = m\,Cp_{BM}\,\Delta T_{BM} \qquad \text{Equation 2}$$

Where m is equal to 1kg of biomass mixture, Cp_{BM} is the specific heat value for the biomass mixture, and ΔT_{BM} is the temperature difference between the ambient temperature and 80°C following Paul and Dutta (2018) observations on the Cp_{BM} behavior.

$$Cp_{BM} = Cp_B\,wt_B + Cp_W\,wt_W \qquad \text{Equation 3}$$

Where Cp_B is the specific heat value for the fiber of interest; values of 2.5, 1.5 and 1.7 KJ Kg^{-1} K^{-1} were considered for SCB, EFB and AB, respectively (References). The ratio of biomass in comparison with the dilute alkali solution (w/w %) wt_B was 9%. Whereas Cp_W is the specific heat value for the dilute alkali solution; for simplicity, the contribution of NaOH to the Cp_W will not be considered. The ratio of dilute alkali solution in relation with the amount of fiber (w/w %) is given by wt_W and was equal to 91%.

The specific heat value for the dilute alkali solution Cp_W (KJ Kg^{-1} K^{-1}) is given by:

$$Cp_W = 0.00001T^2 - 0.0013T + 4.2885 \qquad \textit{Equation 4}$$

Where T is the AHPT temperature.

$$E_W = m\,Cp_W\,\Delta T_W \qquad \textit{Equation 5}$$

Following Paul and Dutta (2018), ΔT_W is given by the difference between the AHPT temperature and 80°C.

The energy produced from LB at the different AHPT conditions in terms of raw fiber was calculated as according to the VS recovered from the AHPT and the BMP achieved in the co digestion of liquid and solid hydrolysates. Energy gain was then calculated as the surplus energy produced by treating LB minus the energy expenditure in the hydrothermal reactor.

4.3Theoretical estimation NaOH recovery

The amount of energy needed for the thermal regeneration of NaOH was calculated according to the shifts in the equilibrium composition of $NaHCO_3$ at different temperatures.

4.4. Analytical methods

4.4.1 Chemical oxygen demand (COD.

Total and soluble COD will be determined according to APHA Standard method 8000 adding the sample to HACH kits (LCK 514). Soluble COD was determined after centrifuging the LH sample for 10 minutes at 1000rpm and filtrating the supernatant through a 0.45µm filter.

4.4.2 pH, conductivity and alkalinity

Samples pH and conductivity were measured with a Multi 9620 IDS multi-parameter whereas alkalinity was measured according to Standard methods (APHA 2008).

4.4.3 Solids fractions

Total solids, total suspended solids, total volatile solids, and total volatile suspended solids were measured according to Standard methods (APHA 2008) 2540 B, D, and E, respectively.

4.4.4 Compositional analysis

The lignin and structural carbohydrates of raw and treated fibers were measured according to the Laboratory Analytical Procedure developed by the National Renewable Energy Laboratory outlined in technical report NREL/TP-510-42618 (2012).

4.4.5 Sugars and degradation products determination in liquid hydrolysate.

The concentration of D-cellobiose, D-(+) glucose, D-(+) xylose, D-(+) galactose, L-(+) arabinose, and D-(+) mannose in the liquid hydrolysates was measured according to NREL-LAP outlined in NREL/TP-510-42623. A Shimadzu high-performance liquid chromatography (HPLC) device equipped with a refractive index detector and a Biorad Aminex HPX-87H column was used. Sulphuric acid 0.005M was used as a mobile phase at a flow rate of 0.5ml per minute. The pH of the samples was adjusted to a value below 3 with 2M sulphuric acid. A sample injection volume of 10µl was used. The column temperature was set at 40°C. A five point calibration curve (0.1mg/L, 0.25mg/L, 0.5mg/L, 0.75mg/L and 1mg/L) was obtained for the different compounds. After applying the best fitting an equation relating compound concentration with its peak area was obtained.

4.4.6 Volatile Fatty Acids

Sludge samples from the manometric BMP test reactors were taken at the beginning and end of the experiments to measure VFA concentration. The samples were centrifuged at 10,000g for 10 min. After this, the samples´ supernatant was filtered through Whatman sterile syringe filters with a pore size of 0.45µm. The samples were diluted 1:10 with internal standard pentanol solution (325.8 mg pentanol/L) and placed in 1.5ml vials. Lastly, 10µl of high purity (>99%) formic acid was added to the samples and mixed thoroughly. The samples were analyzed with an Agilent technologies automatic liquid sampler.

4.4.7 Biogas composition

Biogas samples were analyzed for oxygen, nitrogen, and methane content. The samples were taken with a 1ml syringe and closed with a valve. The biogas samples were injected manually and measured with a micro GC biogas analyzer Agilent 490 (Agilent, Santa Clara, USA) equipped with a 19095P-UO4 molsieve column and an FID detector.

5. RESULTS AND DISCUSSION

5.1 Compositional analysis of SCB, EFB, and AB fibers

The fractionation of the main components of LB determine its potential to be considered a viable feedstock for bioenergy production processes. For instance, Thomsen *et al.*, (2014) employed canonical linear mixture models on 64 different data sets to predict the BMP of lignocellulosic biomass according to its cellulose (x_C), hemicellulose (x_H), lignin (x_L) and residuals (x_R) content. Table 5 shows the variations in the compositional characteristics of SCB, EFB and AB as well as the predicted BMP following equation 6.

$$pBMP = 378x_C + 354x_H - 194x_L + 313x_R \qquad \textit{Equation 6}$$

$$\begin{aligned} &Where: \\ &x_R = 1 - x_C - x_H - x_L \end{aligned}$$

Table 5 Measured ompositional analysis sugarcane bagasse (SCB), empty fruit bunch (EFB), and agave bagasse (AB) following Laboratory Analytical Procedure developed by the National Renewable Energy Laboratory outlined in technical report NREL/TP-510-42618 (2012).

Component (%)	**SCB**	**EFB**	**AB**
Glucans	31	42.8	34.2
Xylan	18.3	25.8	15.6
Arabinan	2.4	1	0.4
Acetyl group	2	5.5	4.3
Klason lignin + ash	36.2	17.5	16.4
Humidity	0.6	1.6	3.7
ND	9.6	5.8	25.4
pBMP (ml CH_4 gVS substrate $^{-1}$)	158	263	257

Cellulose is the main polymer present in all fibers followed by hemicellulose. Lignin content in SCB presents high variation in comparison to that of EFB and AB. The variations in the composition can be attributed to the place, climatic conditions, the type of soil where the biomass grows as well as the harvest season. Likewise, the conditions of the agro industrial process they were part of also influences the compositions. According to Hosseini & Wahid (2015), palm oil production involves the sterilization of fresh fruit bunches at 140°C during 40 minutes which could be considered as a thermal pretreatment. Likewise, the low lignin content in AB could be related with the hydrothermal cooking stage to which agave heads are put through in the tequila production process (Arreola-Vargas *et al.,* 2015).

Following equation 6 we can expect a lower BMP for raw SCB fibers. Studies have shown that lignin has a negative linear correlation with bioenergy production efficiency including methane yield (Liew *et al.,* 2012; Williams *et al.,* 2015). The BMP of pure LB components has been evaluated (Ma *et al.,* 2019; Li *et al.,* 2018); hemicellulose presented a higher hydrolysis rate than cellulose. Nevertheless, cellulose achieved a higher BMP despite its crystallinity since acidification of anaerobic digestion systems due to VFA accumulation occurred in digesters fed with hemicellulose. Both studies agreed that higher BMP can be obtained by co digestion of hemicellulose and cellulose since acidification in the system can be avoided; lignin could not be anaerobically digested. On top of that, lignin creates a barrier for the hydrolysis of carbohydrates thus, opening up the structure of SCB, to make cellulose and hemicellulose available for microorganisms, could be more difficult in comparison with EFB and AB (Ma *et al.,* 2019).

The high variability on compositional characteristics makes it interesting to investigate the effects that the same set AHPT operational conditions has on the sugars release and biomethane potential of SCB, EFB and AB. A range of compositional variations in the SH and LH obtained from AHPT of SCB, EFB and AB can be expected. Cellulose, hemicellulose and lignin can be degraded by AHPT into pentoses, hexoses, and inhibitory compounds which are solubilized in the liquid fraction. The SH (*i.e.,* treated fiber) is, in the best case scenario, mainly composed of cellulose. The compositional characteristics of the SH and LH give an indication of the effects of a certain treatment in the disruption of the lignocellulosic matrix. In the same manner, hydrolysates composition gives an indirect indication of the expected effects in downstream processes.

The study of the interactions of the different sets of operational conditions given by the CCRD with SH and LH specific response variables were tested. For the LH, the concentration of glucose, xylose, arabinose and cellobiose were considered as response variables. For the SH, the solid recovery yield, and the compositional characteristics of the fiber were considered as the response variables. Along with this, the variations in the methane composition of the biogas generated by each conditions was also considered as a response variable. Section 5.2, 5.3 and 5.4 show the effects of AHPT on SCB, EFB and AB, respectively.

5.2 Sugarcane bagasse (SCB) alkaline hydrothermal pretreatment (AHPT).

5.2.1 Effect on liquid hydrolysate (LH) composition

Figure 5 shows the effects of the AHPT operational conditions tested following CCRD (Table 4), on the solubilization of cellulose and hemicellulose fractions of SCB. The concentration of pentoses and hexoses in the LH gives an indication of the LB fraction that is being solubilized by the pretreatment. Variations in the types and concentration of monosaccharides was observed for all the conditions. Glucose was the main monosaccharide present in all conditions and in some cases (C1 to C7, and CP) the only degradation product observed. Xylose and arabinose release was observed for all conditions with +α values (C8, C9, and C14) and conditions with at least two +1 values (C10, C11, and C13). Xylose was present in less quantity than glucose and arabinose.

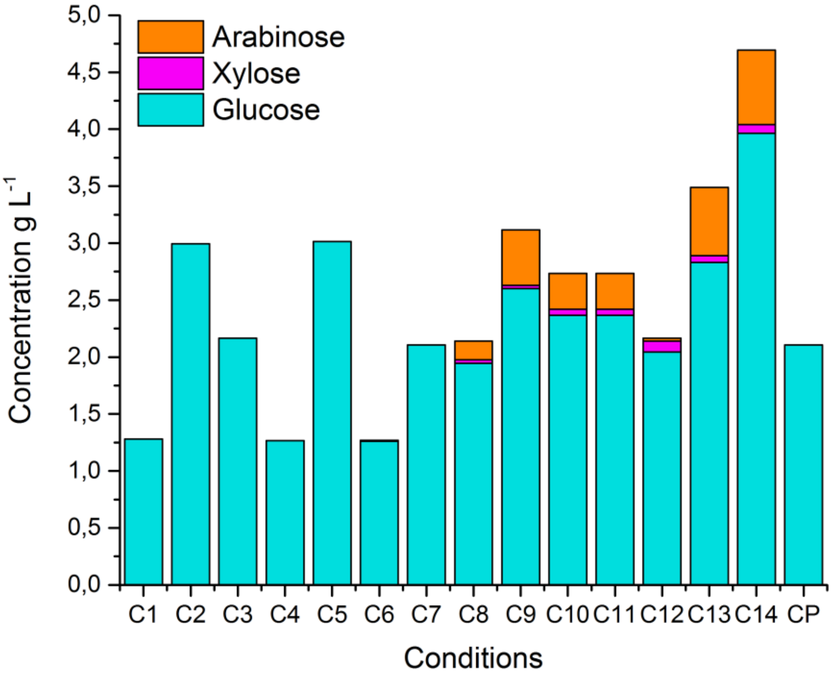

Figure 5 Sugars composition on the liquid fraction recovered from alkaline hydrothermal pretreatment of sugarcane bagasse (%).C1 (146ºC, 1.5M, 20 minutes), C2 (160 ºC, 1M, 10 minutes), C3 (160 ºC, 2M, 30 minutes), C4 (160ºC, 1M, 30 minutes), C5 (160ºC, 2M, 10 minutes), C6 (180 ºC, 0.66M, 20 minutes) C7 (180 ºC, 1.5M, 3.18 minutes), C8 (180 ºC, 1.5 M, 36.82 minutes), C9 (200 ºC, 2.34M, 20 minutes), C10 (200 ºC, 2M, 30 minutes), C11 (200 ºC, 1M, 30 minutes), C12 (200 ºC, 1M, 10 minutes), C13 (200 ºC, 2M, 10 minutes), C14 (213.64 ºC, 1.5M, 20 minutes), CP (180 ºC, 1.5M, 20 minutes)

The application of RSM coupled with CCRD served as a tool to determine the significance in the interactions between the operational conditions and the response variables of interest in the LH (glucose, xylose, and arabinose concentration).

Temperature (ºC) and NaOH concentration (M) had a significant positive linear effect (p-value <0.05) on glucose release from SCB (Figure 31). Temperature shows a higher effect when compared with NaOH. Thus, it can be inferred that NaOH loading can be reduced by increasing temperature. A model was predicted with CCRD (Equation 7) indicating the linear effect of temperature (ºC) and NaOH concentration (M) on glucose release.

$$\text{Glucose}_{SCB} = 2.29 + 0.34x_1 + 0.29x_2 \qquad \text{Equation 7}$$

The coefficient of determination R^2 was used to test the accuracy of the model. A value of 36.10% was found which suggest a poor fit.

The linear effect of temperature with glucose agrees with findings from Rocha *et al.*, 2013 who found that glucose concentration increased from 0.5g L^{-1} to 1.2g L^{-1} when SCB was hydrothermally pretreated at 180°C and 195°C, respectively. Contrarily to Rocha *et al.*, (2013) glucose was the main monosaccharide found in the LH from SCB in this study. This can be attributed to a higher accessibility to cellulosic compounds due to the delignification effect of NaOH. Van der Pol *et al.*, 2015 found that both cellulose and hemicellulose are affected by AHPT whereas hydrothermal pretreatment affects only the hemicellulose fraction. This study is in agreement with findings from Kumari & Das (2015) who found that glucose is the main monosaccharide present in the LH from SCB undergoing AHPT; its concentration increases with treatment severity.

2D and 3D response surface plots show the interactions for two independent variables while keeping the other variable at CP. Figure 6 shows the interactions of temperature (°C) and NaOH (M) on glucose release from SCB. The linear interaction between temperature and NaOH indicates that it still might be possible to increase the glucose concentration in the hydrolysates by increasing the upper values (+1) of these values. However, attention should be paid since at higher treatment severities the formation of inhibitory compounds increases (Lobo-Baeta *et al.*, 2016).

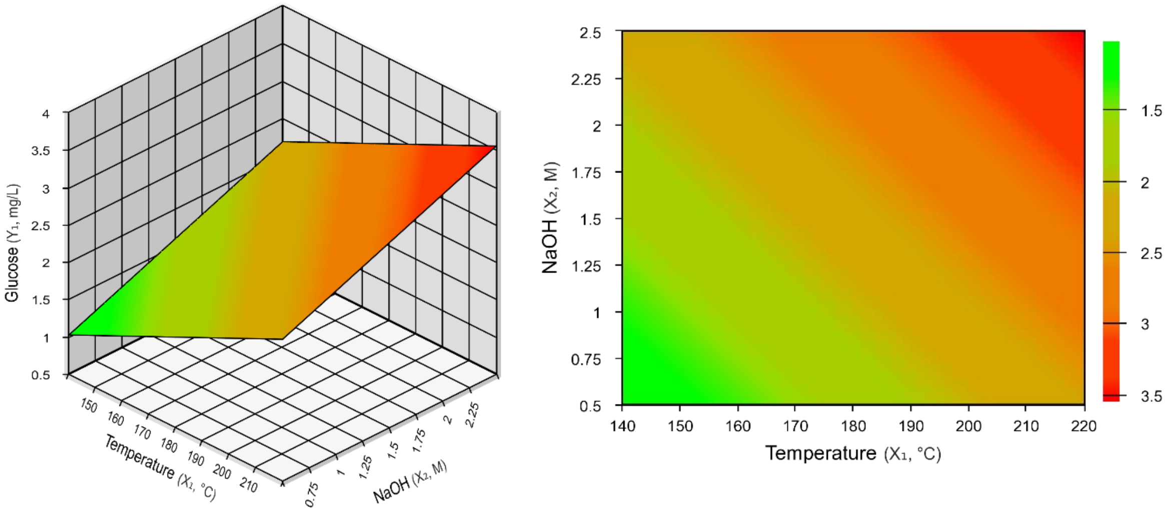

Figure 6 Response surface 3D and 2D plots indicating the effect of the interaction between x1: temperature (ºC) and x2: NaOH concentration (M) for glucose release from sugarcane bagasse (SCB) undergoing alkaline hydrothermal pretreatment.

Temperature (ºC) and NaOH concentration (M) had a significant positive linear effect (p-value <0.05) on arabinose release from SCB. Temperature shows a higher effect when compared with NaOH (Figure 32). A model was predicted with CCRD (Equation 8) indicating the different interactions of the independent variables with arabinose release from SCB.

$$\text{Arabinose}_{SCB} = 0.17 + 0.17x_1 + 0.10x_2$$ *Equation 8*

The coefficient of determination R^2 was used to test the accuracy of the model. A value of $R^2 = 67.38$ was found, this is the model presents a good fit with the observed responses.

The linear interaction between temperature and arabinose release can be attributed to the release of acetic acid at high temperatures due to the degradation of acetyl groups that are present in hemicellulose (Jönsson and Martín, 2016). Acetic acid concentration influences hemicellulose depolymerization by acting as catalyst for the hydrolysis of ester and eter bounds found in hemicellulose (Costa *et al.*, 2014). This is in agreement with Baeta *et al.*, (2016^b) who found that an increase in temperature and treatment time on hydrothermal pretreatment of SCB contributes to a higher release of pentoses (xylose and arabinose) due to hemicellulose hydrolysis. However, they also specified that conditions that lead to a high dissolution of hemicellulose are not necessarily the best for methane production since hydrolysates could contain anaerobic digestion inhibitory compounds (Baeta *et al.*, 2016[b]). Rocha *et al.*, 2013 found that hemicellulose release not only increases with temperature but also with the non-isothermal heating phase of the reactor, considering that longer times are required to reach +1 and +α values for temperature it is reasonable to have higher arabinose concentrations at these points.

Figure 7 shows 2D and 3D response surface plots for the significant interactions of temperature (°C), NaOH (M) on arabinose release from SCB. The linear interaction between temperature and NaOH indicates that it still might be possible to increase the glucose concentration in the hydrolysates by increasing the upper values (+1) of these values. However, attention should be paid since at higher treatment severities the formation of inhibitory compounds increases (Lobo-Baeta *et al.*, 2016).

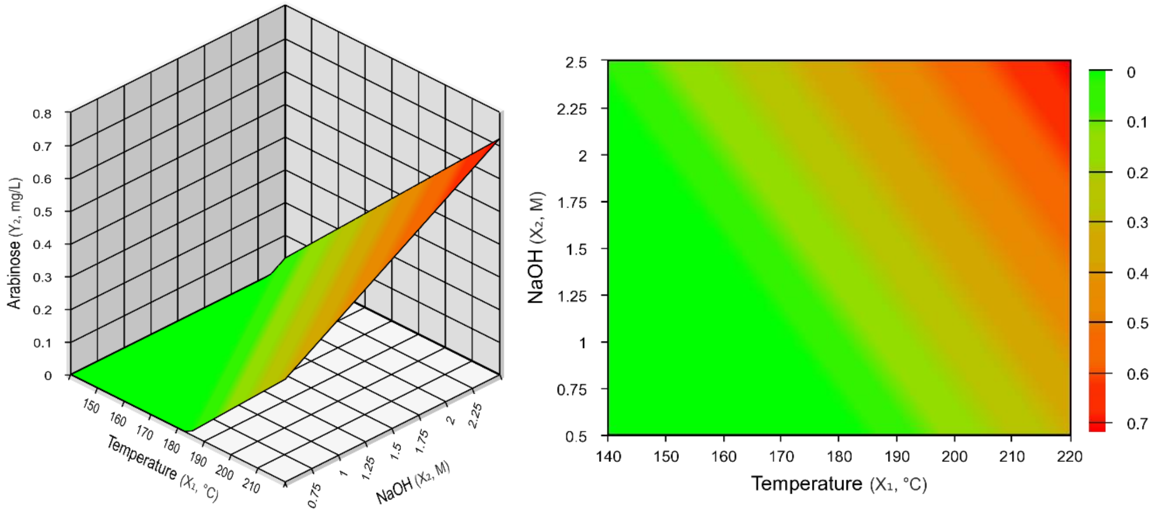

Figure 7 Response surface 3D and 2D plots indicating the effect of the interaction between: a) x1: temperature (ºC) and x2: NaOH concentration (M) b) x1: temperature (ºC) and x3: Retention time c for arabinose release from sugarcane bagasse (SCB).

Contrary to the glucose and arabinose release, the independent variables were not statistically significant for xylose release at the tested levels.

5.3.1 Effect on solid hydrolysate composition

Figure 8 shows the changes in the compositional contents of SCB fiber as a result of AHPT. Lignin and carbohydrates content where affected by the pretreatment. Cellulose (glucan), hemicellulose (xylan and arabinan) and lignin are present in all conditions. The lower lignin content was observed in C10 (200 ºC, 2M, 30 minutes) which is a combination of high values (+1) in the independent variables. Low lignin content was also observed on C13 (7.08%), C11 (8.62%), C9 and C14 (9.09%). C9 and C14 involve a +α value for NaOH and temperature, respectively. Whereas C11 and C13 involve two conditions with +1 values; temperature and time for C11 and temperature and NaOH for C13. This indicates that at high temperature and NaOH values, higher delignification of SCB fibers can be expected.

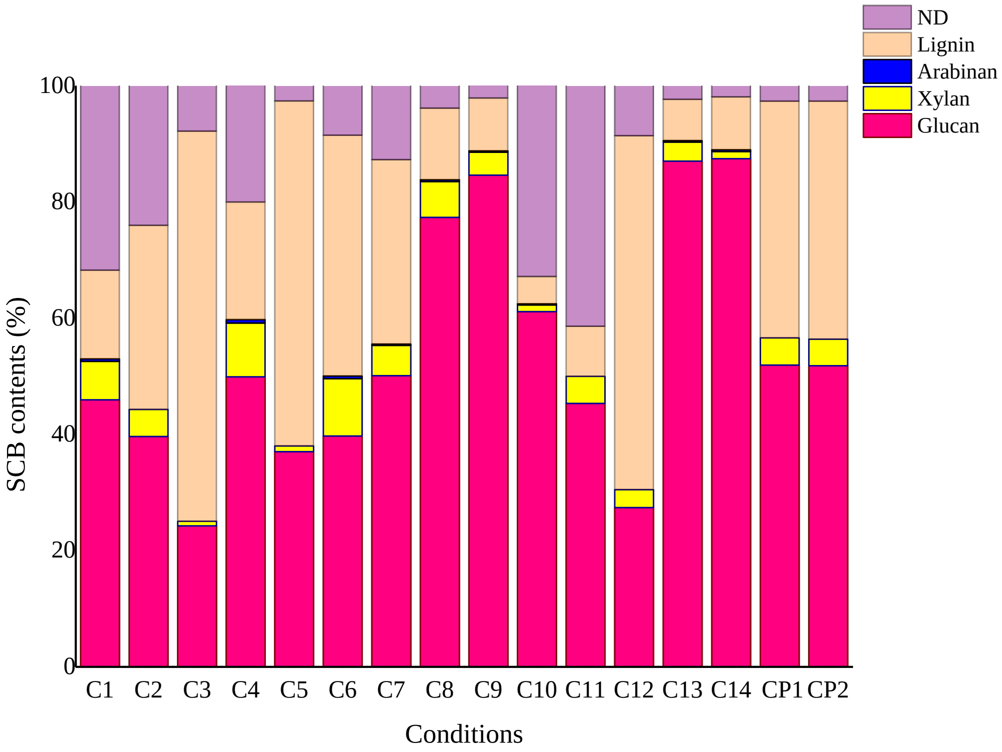

Figure 8 Sugars composition on the solid fraction recovered from alkaline hydrothermal pretreatment of sugarcane bagasse (%). C1 (146.36 ºC, 1.5M, 20 minutes), C2 (160ºC, 1M, 10 minutes), C3 (160ºC, 2M, 30 minutes), C4 (160 ºC, 1M, 30 minutes), C5 (160 ºC, 2M, 10 minutes), C6 (180ºC, 0.66M, 20 minutes), C7 (180 ºC, 1.5M, 3.18 minutes), C8 (180 ºC, 1.5M, 36.82 minutes), C9 (180 ºC, 2.34 M, 20 minutes), C10 (200 ºC, 2M, 30 minutes), C11 (200 ºC, 1M, 30 minutes), C12 (200 ºC, 1M, 10 minutes), C13 (200ºC, 2M, 10 minutes), C14 (213.64 ºC, 1.5M, 20 minutes), CP (180 ºC, 1.5M, 20 minutes).

Cellulose content (measured as glucan) was maximum at C13 which includes two conditions with +1 values, temperature and NaOH. Likewise, cellulose content in the fibers was high for conditions 14, 9 and 8 which include +α values for temperature, NaOH and retention time, respectively. Therefore, cellulose exposure on SCB fibers can be expected to increase at higher treatment severities. This is in agreement with Carrillo *et al.*, (2017) who found that increasing retention time resulted in a higher glucan content and reduced xylan content in the SH.

Temperature (ºC) and NaOH concentration (M) have a significant (p-value <0.05) effect on SCB fibers lignin content (Figure 33). Some studies (Antonopoulou & Lyberatos 2013; Sambusiti *et al.*, 2013) have concluded that NaOH alone does not contribute to sugars solubilization nor to delignification of lignocellulosic biomass but the interaction between alkali concentration and temperature. A model was predicted with CCRD (Equation 9) indicating a linear effect of temperature (ºC) and NaOH concentration (M) on the SCB fibers delignification.

$$\text{Lignin content}_{\text{SCB}} = 28.78 - 16.55 x_1 x_2 \qquad \text{Equation 9}$$

Delignification is considered as the principal objective for lignocellulosic biomass pretreatment since a lower lignin content leads to an increase in methane production (Carrere *et al.*, 2016). According to equation 9, a higher temperature and NaOH concentration would lead to a lower lignin content in the solid hydrolysate which can be attributed to degradation into phenolic compounds due to rupture of the ester bonds (Costa *et al.*, 2014).

Figure 9 shows the interactions of temperature (°C) and NaOH (M) on SCB delignification.

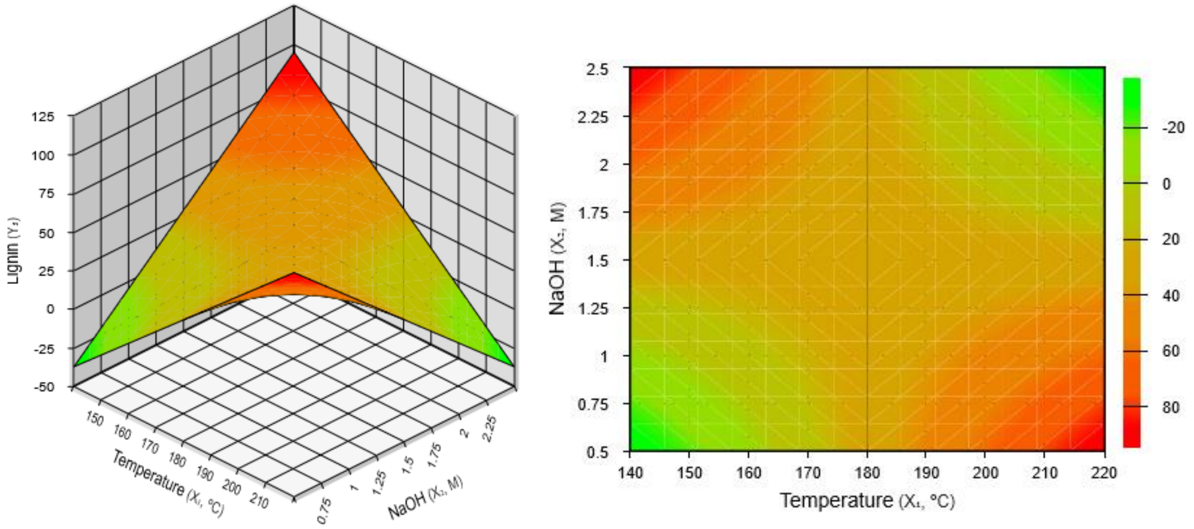

Figure 9 Response surface 3D and 2D plots indicating the effect of the interaction between x_1: temperature (ºC) and x_2: NaOH concentration (M) on delignification of sugarcane bagasse (SCB) undergoing alkaline hydrothermal pretreatment

Solids recovery from alkaline pretreated sugarcane bagasse (SCB).

Temperature (°C), NaOH concentration (M), its coupled effect as well as retention time (min), have a significant negative linear effect ($p\text{-value} < 0.05$) on solids recovery from SCB which is an indication that fiber solubilization increases along with the severity of the pretreatment (Figure 30). A model was predicted with CCRD (Equation 10) indicating the independent variables and their interactions on solids recovery from SCB.

$$\text{Solids recovery}_{SCB} = 10.68 - 2.60x_1 - 2.63x_2 - 1.96x_3 + 2.52x_3^2 - 2.40x_1x_2 \qquad \textit{Equation 10}$$

The coefficient of determination R^2 was used to test the accuracy of the model. A value of $R^2 = 80.59\%$ was found.

2D and 3D response surface plots showing the interactions between the independent variables are presented in Figure 10

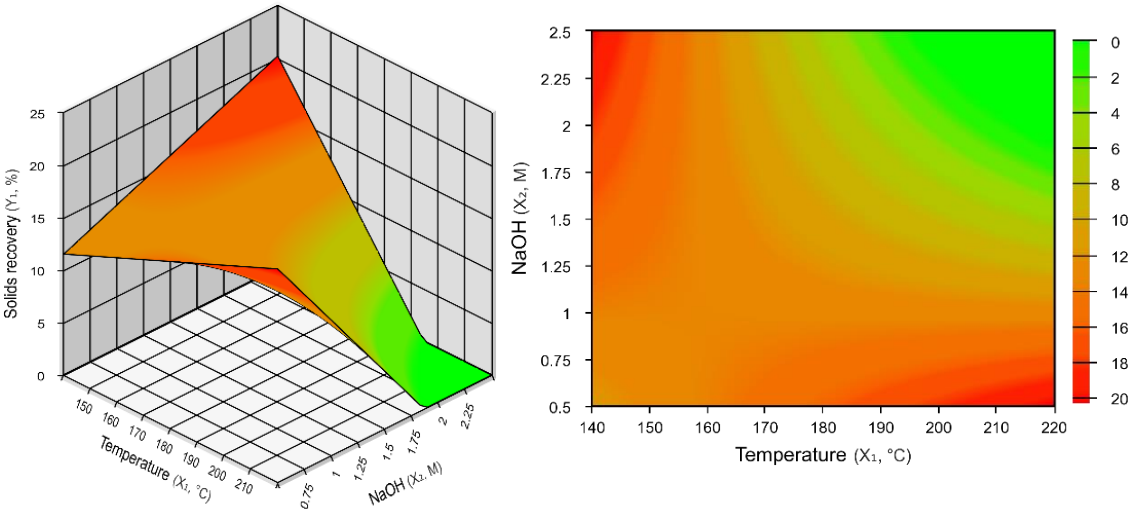

Figure 10 Response surface 3D and 2D plots indicating the effect of the interaction between: x1: temperature (°C) and x2: NaOH concentration (M) for solids recovery from sugarcane bagasse (SCB)

5.2.3 Effect on biomethane potential (BMP).

Manometric BMP test were carried out according to section 4.3.3. Table 6 shows the BMP potential of raw and treated sugarcane bagasse. The BMP potential varied among mono and co digestion of the SH and LH. Mono digestion of SH obtained at CP AHPT conditions (180°C, 1.5M NaOH, 20min) resulted in an increase of methane production from 112 to 318 ml CH_4 gVS^{-1} in comparison with the raw fiber this can be attributed to the higher exposure of cellulose as a result of delignification and hemicellulose solubilization. On the other hand, mono digestion of the LH obtained at CP AHPT conditions (180°C, 1.5M NaOH, 20min) resulted in a decrease on methane production in comparison with the raw fiber yielding only 44 ml CH_4 gVS^{-1} this suggest that anaerobic digestion inhibitory compounds formed from degradation of pentoses and hexoses might have been present in the LH. Co digestion of the liquid and solid hydrolysates resulted in a methane production of 164 ml CH_4 gVS^{-1} in comparison to the raw fiber 112 ml CH_4 gVS^{-1} which suggest that the SH helped in the mitigation of the inhibitory effects from LH.

Table 6 Biomethane potential (BMP) of raw and alkaline hydrothermal pretreatment sugarcane bagasse (SCB) hydrolysates at central point (CP) conditions (180°C, 1.5M NaOH, 20min).

	BMP (ml CH_4 gVS^{-1})
Raw SCB	112
CP co digestion hydrolysates	164
CP solid hydrolysate	318
CP liquid hydrolysate	44

Retention time presented a significant (p-value <0.05) negative quadratic interaction with the BMP of SCB undergoing AHPT whereas NaOH presented a significant (p-value <0.05) positive linear effect (Figure 31). A model was predicted with CCRD (Equation 11) indicating the linear and quadratic effect of temperature (ºC) and retention time (min) on the biomethane potential of SCB, respectively.

$$BMP_{SCB} = 162.36 + 28.87x_2 - 37.84x_3^2 \qquad \textit{Equation 11}$$

The coefficient of determination R^2 was used to test the accuracy of the model. A value of $R^2 = 40.27$ was found.

2D and 3D response surface plots (Figure 11) show the interactions of time (min) and NaOH (M) on BMP from SCB.

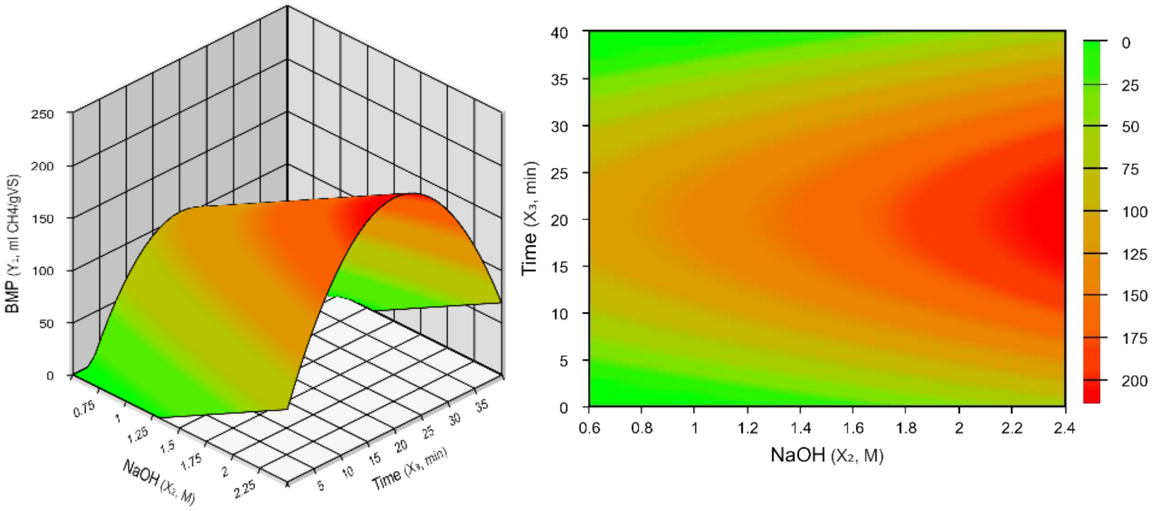

Figure 11 Response surface 3D and 2D plots indicating the effect of the interaction between x2: NaOH concentration (M) and x3: Retention time (min) on biomethane potential (BMP) from co digestion of sugarcane bagasse (SCB) hydrolysates

5.2.4 Effect on methane content in biogas.

Temperature (ºC), and NaOH concentration (M) have a significant linear effect (p-value <0.05) on methane content in biogas produced from co digestion of AHPT SCB hydrolysates (Figure 36). A model was predicted with CCRD (Equation 12) indicating the linear effect of temperature (ºC) and NaOH concentration (M) on the methane content in biogas produced from pretreated SCB.

$$\text{Methane content}_{SCB} = 47.44 + 8.63x_1 + 6.28x_2$$ *Equation 12*

The model (Equation 12) fitted to the data cover more than 50% of the data (R^2 = 62.84%).

2D and 3D response surface plots (Figure 12) show the interactions of temperature (°C) and NaOH (M) on methane content in biogas produced from co digestion of AHPT SCB hydrolysates.

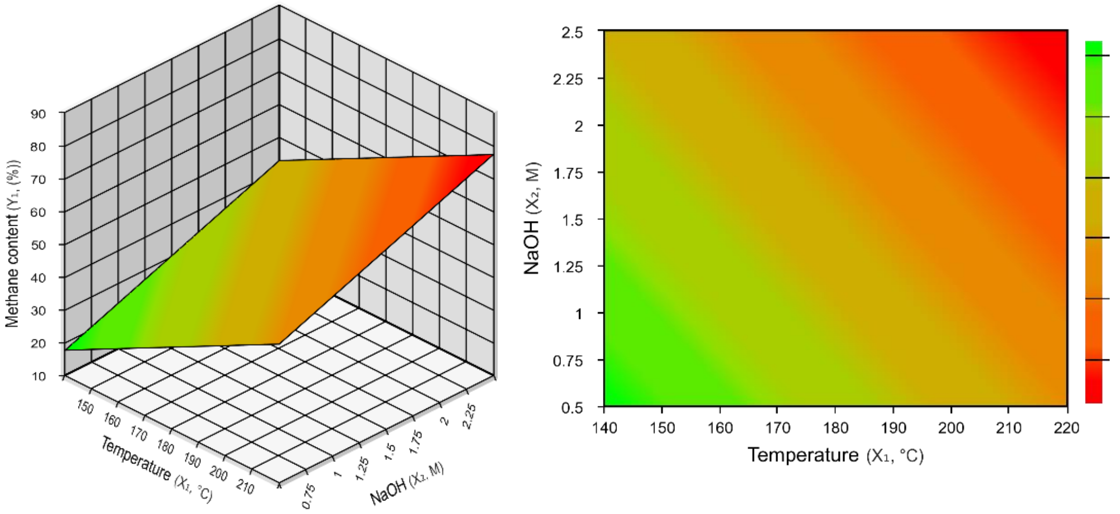

Figure 12 Response surface 3D and 2D plots indicating the effect of the interaction between x_1: temperature (ºC) and x_2: NaOH concentration (M) on methane content from co digestion of sugarcane bagasse (SCB) hydrolysates.

5.3 Empty fruit bunch (EFB) alkaline Hydrothermal pretreatment (AHPT).

5.3.1 Effect on liquid hydrolysate (LH) composition

An indication of AHPT effect on the solubilization of cellulose and hemicellulose components is shown in Figure 13. The concentration of glucose gives an indication of cellulose degradation whereas arabinose and xylose are degradation products from hemicellulose. The presence of the different monosaccharides was variable in terms of type and concentration for all the conditions tested following CCRD. For instance, glucose was present in all conditions indicating that the cellulose fraction is affected by alkaline hydrothermal pretreatment. Glucose was present in all conditions and in some cases (C1-C6, C11 and C12) it was the main degradation product observed. Arabinose release was observed for all conditions at a higher concentration in +1 and +α values for temperature and residence time. Xylose was present in all conditions whereas cellobiose was only detected in hydrolysates in some conditions (C2, C4, C6, C12, and C14).

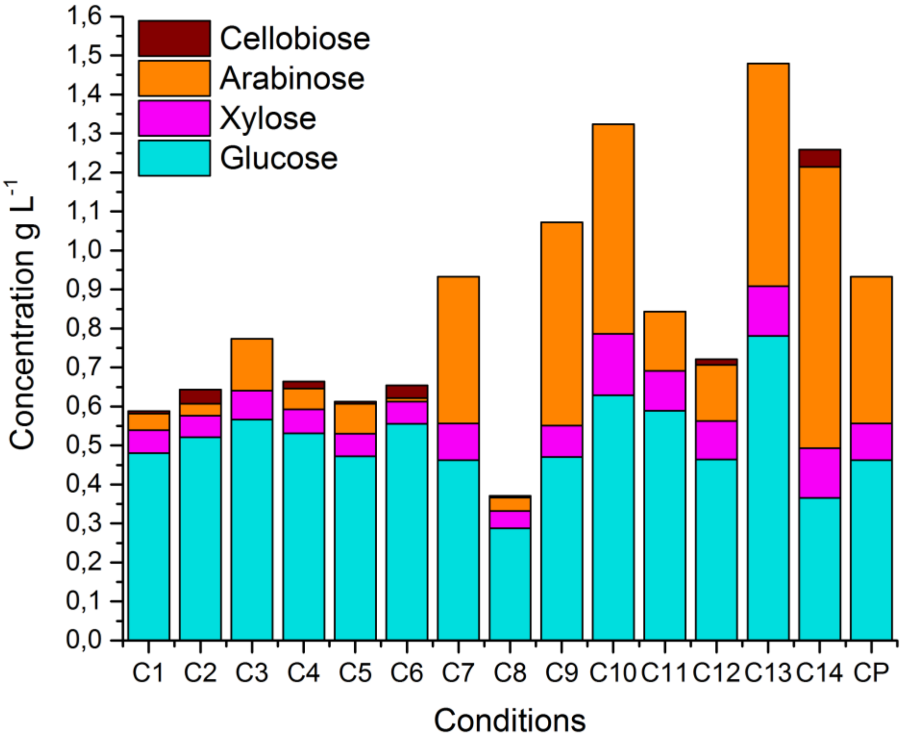

Figure 13 Sugar released from empty fruit bunches as a function of different conditions of alkaline hydrothermal pretreatment C1 (146ºC, 1.5M, 20 minutes), C2 (160 ºC, 1M, 10 minutes), C3 (160 ºC, 2M, 30 minutes), C4 (160ºC, 1M, 30 minutes), C5 (160ºC, 2M, 10 minutes), C6 (180 ºC, 0.66M, 20 minutes) C7 (180 ºC, 1.5M, 3.18 minutes), C8 (180 ºC, 1.5 M, 36.82 minutes), C9 (200 ºC, 2.34M, 20 minutes), C10 (200 ºC, 2M, 30 minutes), C11 (200 ºC, 1M, 30 minutes), C12 (200 ºC, 1M, 10 minutes), C13 (200 ºC, 2M, 10 minutes), C14 (213.64 ºC, 1.5M, 20 minutes), CP (180 ºC, 1.5M, 20 minutes)

Temperature (ºC) and time (min) had a significant p-value <0.05) quadratic and linear effect on glucose release from EFB, respectively (Figure 37). A model was predicted with CCRD (Equation 13) indicating the quadratic effect of temperature (ºC) and retention time (min) on glucose release.

$$\text{Glucose}_{EFB} = 0.63 - 0.06\, x_1^2 - 0.07 x_3^2 \qquad \textit{Equation 13}$$

The model (Equation 7) fitted to the data cover more than 50% of the data (R^2 = 34.39%).

It has been observed that even when glucan content in the pretreated SH increases with the severity of pretreatment conditions, the absolute glucan recovery decreases since a portion of cellulose is also degraded into glucose and/or inhibitory compounds (Han *et al.*, 2011). Perdana *et al.*, 2019 studied the effects of microwave power (W), NaOH (%w/v) concentration and retention time (min) on lignin removal from microwaved assisted AHPT EFB. They used a Box-Behnken design (BBD) in order to determine the best treatment conditions and found a significant positive linear effect between microwave power and retention time and a quadratic effect of NaOH with lignin removal. The optimal point for lignin removal was found at the higher levels of the operational, conditions (832.9 W, NaOH concentration of 2.7% (w/v), and a reaction time of 8.9 min). This is, higher pretreatment severities allow for higher lignin removal which results in increased solubilization of the cellulose and hemicellulose fractions of EFB fibers which agrees with findings in the current study.

Figure 14 shows the interactions of temperature (°C) and retention time (min) on glucose release from EFB. An optimization on glucose release can be achieved thanks to the quadratic interaction between temperature and retention time. It can be observed that a maximum glucose yield is achieved at the CP conditions (180°C, 1.5M, 20min). If treatment severity is increased, the glucose concentrations decreases due to further degradation into 5-HMF.

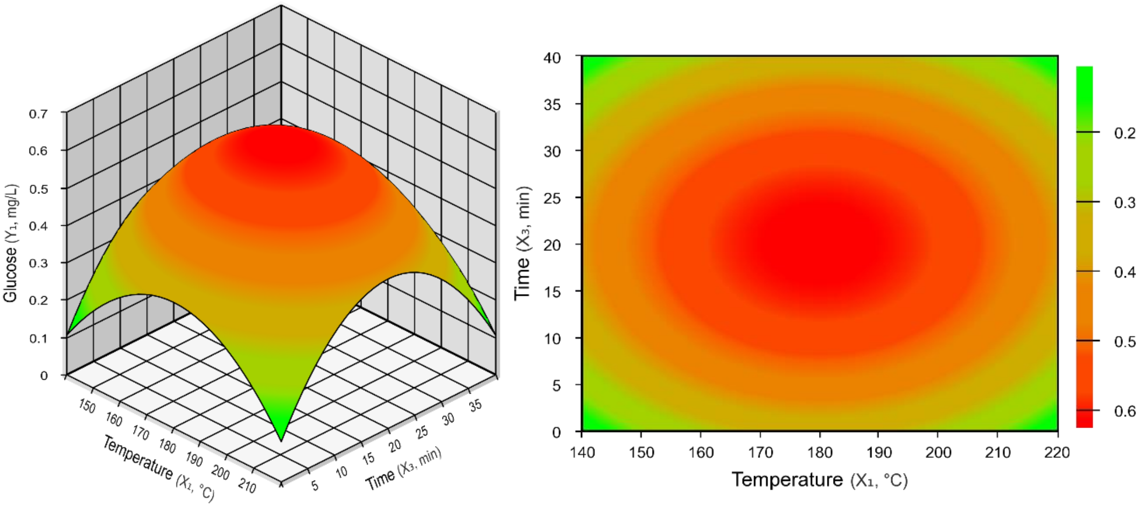

Figure 14 Response surface 3D and 2D plots indicating the effect of the interaction between x1: temperature (°C) and x3: time (min) for glucose release from empty fruit bunch (EFB)

Temperature (°C) and NaOH concentration (M) had a significant (p-value <0.05) positive linear on arabinose release from EFB. Temperature has the higher influence followed by NaOH concentration (Figure 38). A model was predicted with CCRD (Equation 14) indicating the effect of temperature (°C), NaOH concentration (M) arabinose release from EFB.

$$\text{Arabinose}_{EFB} = 0.25 + 0.16x_1 + 0.13x_2 \qquad \textit{Equation 14}$$

The coefficient of determination R^2 was used to test the accuracy of the model. A value of 74.93% was found.

A linear effect of NaOH concentration with hemicellulose solubilization from EFB was reported by Kim (2018). In such study, the amount of hemicellulose in the SH treated at 121°C during 60min decreased from 19.7g to 4.9g when dilute alkali conditions (NaOH 3M) where applied.

Plots from Figure 15 show the interactions of temperature (°C) and NaOH (M) on arabinose release from EFB. The linear relation does not allow for an optimization of the process in terms of arabinose release; if the severity of these parameters is increased, higher arabinose release could be observed. However, this will be true up to certain extent after which further degradation into inhibitory compounds will occur.

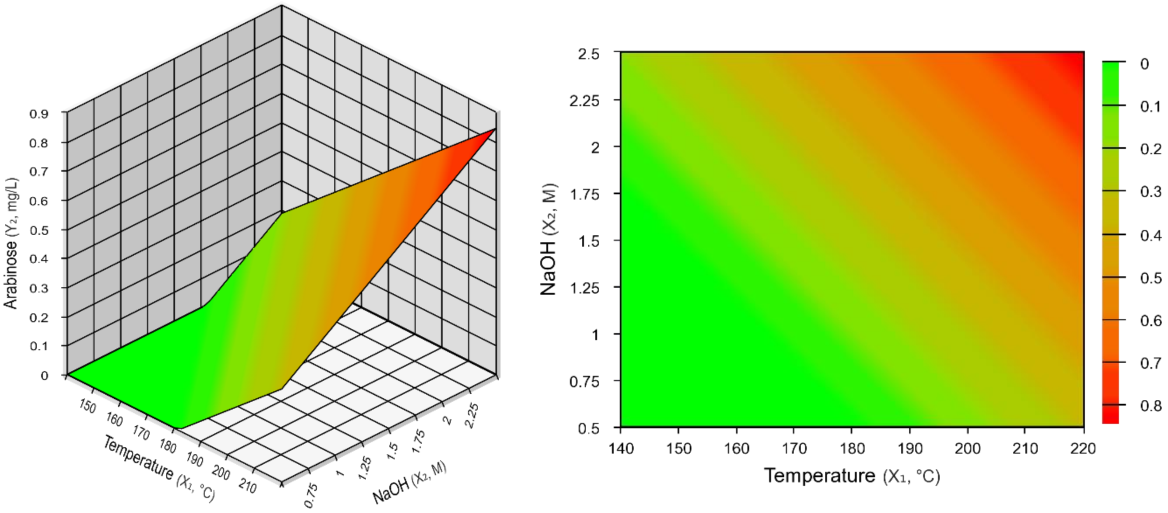

Figure 15 Response surface 3D and 2D plots indicating the effect of the interaction between x1: temperature (ºC) and x2: NaOH concentration (M) for arabinose release from empty fruit bunch (EFB)

Hong *et al.*, 2013 mentioned a different behavior for glucose and arabinose release from EFB pretreated with H_2SO_4 at different concentrations (%w/v) and temperatures. They found that glucose release increases with treatment severity whereas arabinose release reaches a maximum at 160°C, 1.5% (w/v H_2SO_4) and 5 minutes of retention time after which, degradation products started to form at high rate. This can be attributed to the lower delignification capacity of acid pretreatments in comparison with alkaline pretreatments.

5.3.2 Effect on solid hydrolysate.

Temperature (ºC) and NaOH concentration (M) had a significant (p-value <0.05) negative linear effect on solids recovery from EFB (Figure 35). Since the determination of the individual components for the SH was not carried out, solids recovery was used as an indirect indication for LB degradation. A model was predicted with CCRD (Equation 10) indicating the linear effect of temperature (ºC) and NaOH concentration (M) on solids recovery (%) from EFB.

$$\text{Solids recovery}_{EFB} = 28.18 - 7.42x_1 - 4.85x_2 \qquad \textit{Equation 15}$$

The coefficient of determination R^2 was used to test the accuracy of the model. A value of $R^2 = 85.29\%$ was found.

2D and 3D response surface plots (Figure 16) show the interactions of temperature (°C) and NaOH (M) on solids recovery from empty fruit bunch.

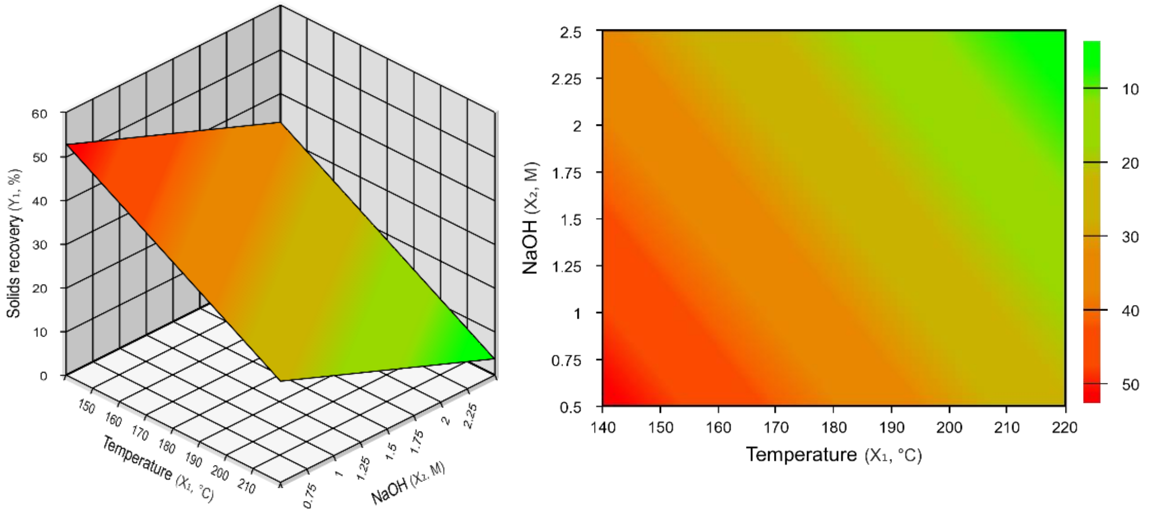

Figure 16 Response surface 3D and 2D plots indicating the effect of the interaction between x1: temperature (ºC) and x2: NaOH concentration (M) on solids recovery from empty fruit bunch (EFB)

5.3.3 Effect on biomethane potential (BMP).

Manometric BMP test were carried out according to section 4.3.3. Table 7 shows the BMP potential of raw and treated EFB. The BMP potential varied among mono and co digestion of the SH and LH. Mono digestion of EFB SH and LH obtained at CP AHPT (180°C, 1.5M NaOH, 20min) resulted in a lower methane production in comparison with the raw fiber. Co digestion of SH and LH resulted in an increase in methane production from 195 to 403 ml CH_4 gVS^{-1} in comparison to the raw fiber.

Table 7 Biomethane potential (BMP) of raw and alkaline hydrothermal pretreatment empty fruit bunch (EFB) hydrolysates at central point (CP) conditions (180°C, 1.5M NaOH, 20min).

	BMP (ml CH_4 gVS^{-1})
Raw EFB	195
CP co digestion hydrolysates	403
CP solid hydrolysate	113
CP liquid hydrolysate	191

Temperature (°C) showed significant (p-value <0.05) negative linear and quadratic interactions with BMP of EFB whereas NaOH presented a significant (p-value <0.05) negative linear effect (Figure 36). A model was predicted with CCRD (Equation 16) indicating that the linear and quadratic effect of NaOH concentration (M) as well as the quadratic effect of temperature (°C) have a negative effect on BMP from co digestion of EFB AHPT hydrolysates.

$$BMP_{EFB} = 396.82 - 41.60x_1^2 - 43.43x_2 - 44.08x_2^2 \qquad \textit{Equation 16}$$

The coefficient of determination R^2 was used to test the accuracy of the model. A value of $R^2 = 47.70$ was found.

Figure 17 shows 2D and 3D response surface plots for the interactions of temperature (°C) and NaOH (M) on BMP from co digestion of EFB AHPT hydrolysates.

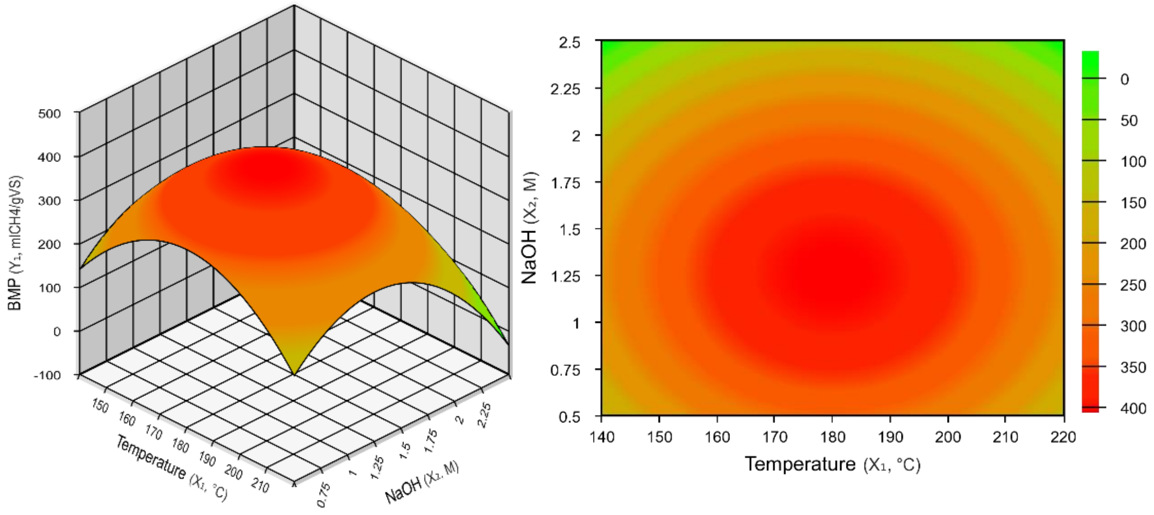

Figure 17 Response surface 3D and 2D plots indicating the effect of the interaction between X_1: temperature (°C) and X_2: NaOH concentration (M) on biomethane potential (BMP) from co digestion of empty fruit bunch (EFB) hydrolysates

5.3.4 Effect on methane content in biogas.

All the independent variables presented a significant (p-value <0.05) quadratic negative interaction with the methane content in biogas produced from co digestion of EFB undergoing AHPT whereas temperature and NaOH concentration presented a significant (p-value <0.05) positive linear effect (Figure 41) . The model (Equation 17) fitted to the data cover close to 90% of the data ($R^2 = 88.08\%$).

$$\text{Methane content}_{EFB} = 81.91 + 5.49x_1 - 7.18x_1^2 + 4.92x_2 - 6.71x_2^2 - 8.35x_3^2 \qquad \textit{Equation 17}$$

2D and 3D response surface plots (Figure 18) show the interactions of the independent variables methane content in biogas produced from co digestion of EFB AHPT hydrolysates.

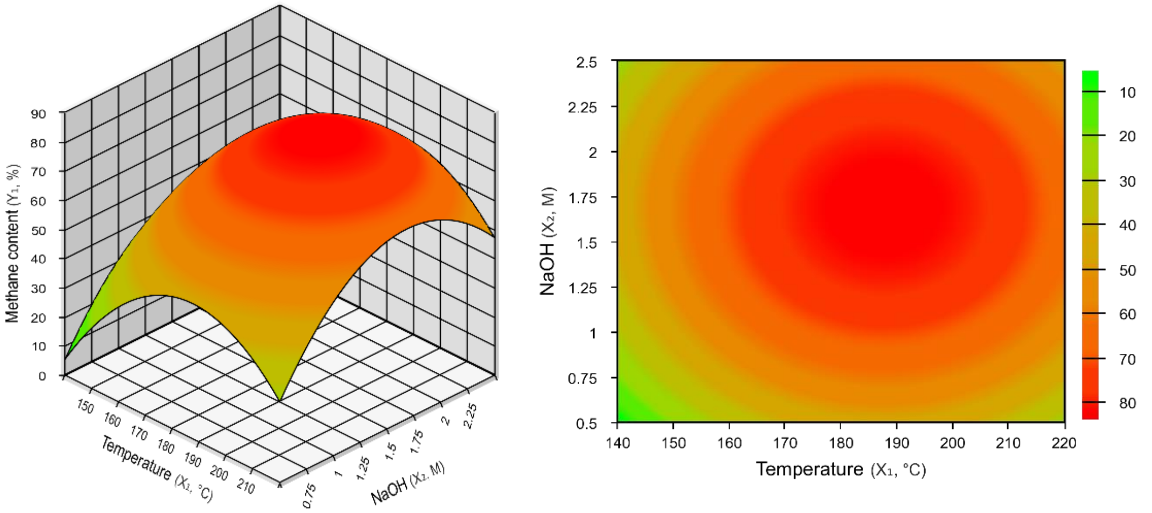

Figure 18 Response surface 3D and 2D plots indicating the effect of the interaction between: a) X_2: NaOH concentration and X_3: Retention time b) X_1: temperature (ºC) and X_3: Retention time and c) X_1: temperature (ºC) and X_2: NaOH concentration (M) on methane content from co digestion of empty fruit bunch (EFB) hydrolysates

5.4 Agave bagasse (AB) alkaline Hydrothermal pretreatment (AHPT)

5.4.1 Effect on liquid hydrolysate (LH) composition

Figure 19 shows the effects of AHPT on the cellulose and hemicellulose fractions of AB. The concentration of pentoses and hexoses in the LH give an indication of the LB fraction that is being solubilized by the pretreatment. The composition of the sugar matrix in the LH changed along with the different operational conditions tested. Glucose, xylose and arabinose were present in all conditions. The concentration of hemicellulose degradation products (xylose and arabinose) was higher than that of cellulose degradation products (glucose). This indicates that hemicellulose was more prone to solubilization than cellulose.

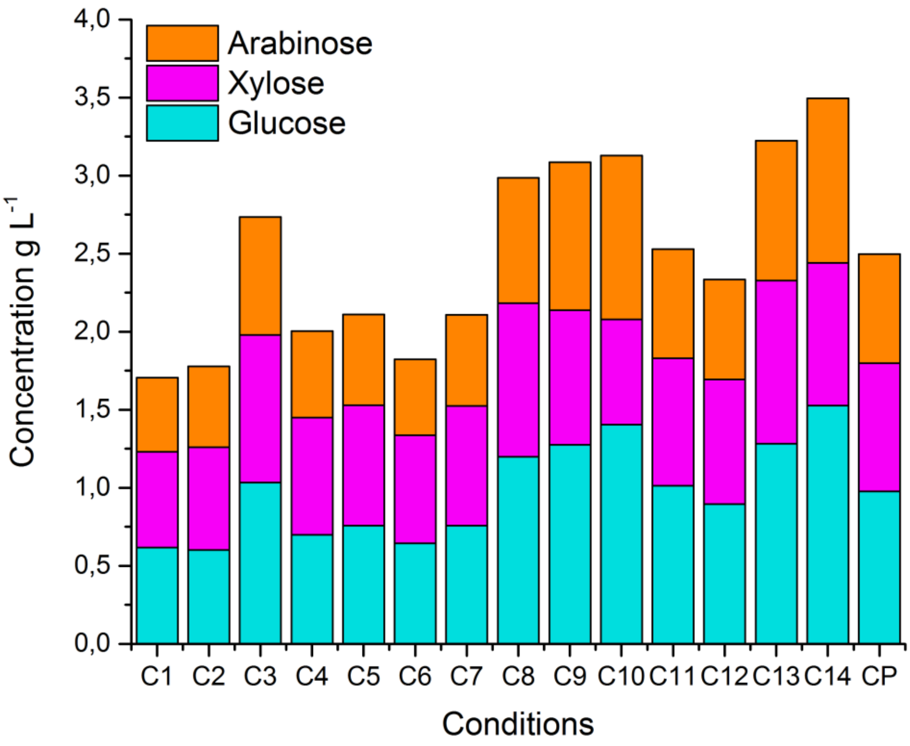

Figure 19 Sugars composition on the liquid fraction recovered from alkaline hydrothermal pretreatment of agave bagasse (%).C1 (146ºC, 1.5M, 20 minutes), C2 (160 ºC, 1M, 10 minutes), C3 (160 ºC, 2M, 30 minutes), C4 (160ºC, 1M, 30 minutes), C5 (160ºC, 2M, 10 minutes), C6 (180 ºC, 0.66M, 20 minutes) C7 (180 ºC, 1.5M, 3.18 minutes), C8 (180 ºC, 1.5 M, 36.82 minutes), C9 (200 ºC, 2.34M, 20 minutes), C10 (200 ºC, 2M, 30 minutes), C11 (200 ºC, 1M, 30 minutes), C12 (200 ºC, 1M, 10 minutes), C13 (200 ºC, 2M, 10 minutes), C14 (213.64 ºC, 1.5M, 20 minutes), CP (180 ºC, 1.5M, 20 minutes)

Temperature (ºC), NaOH concentration (M) and retention time (min) had a significant (p-value <0.05) positive linear effect on glucose release from AB which is an indication that glucose release increases along with treatment severity and NaOH concentration. Temperature has the higher influence followed by NaOH concentration and time (Figure 38). Thus, by increasing treatment temperature, NaOH consumption and or retention time could be decreased while still obtaining a high recovery. A model was predicted with CCRD (Equation 18) indicating the linear effect of temperature (ºC), NaOH concentration (M) and time (min) on glucose release from AB undergoing AHPT fibers.

$$\text{Glucose}_{AB} = 0.98 + 0.22x_1 + 0.17x_2 + 0.10x_3$$ *Equation 18*

The model (Equation 18) fitted to the data cover more than 50% of the data ($R^2 = 93.87\%$).

2D and 3D response surface plots show the interactions for two independent variables while keeping the other variable at CP. Figure 20 shows the interactions of temperature (°C), NaOH (M) and retention time (min) on glucose release from AB. The linear interaction between these variables indicates that it still might be possible to increase the glucose concentration in the hydrolysates by increasing the upper values (+1). However, attention should be paid since at higher treatment severities the formation of inhibitory compounds increases (Lobo-Baeta *et al.,* 2016).

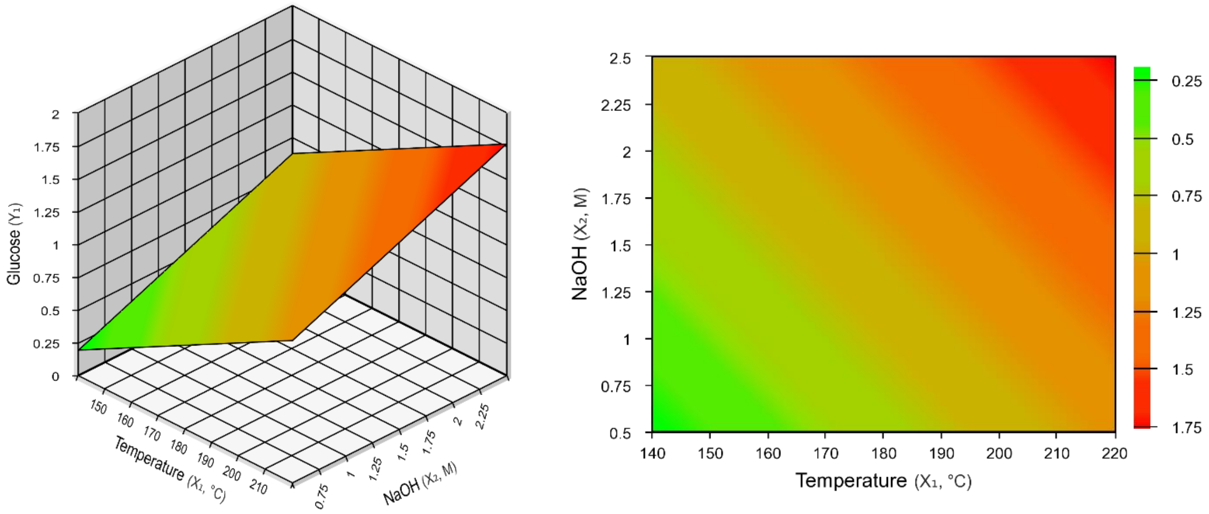

Figure 20 Response surface 3D and 2D plots indicating the effect of the interaction between x1: temperature (ºC) and x2: NaOH concentration (M) on glucose release from agave bagasse

No significant interaction between the independent variables and the xylose concentration in the liquid hydrolysate was found.

Temperature (ºC), NaOH concentration (M), retention time (min) and the interaction between the first two has a significant positive linear effect (p-value <0.05) on arabinose release from AB which is an indication that glucose release increases along with treatment severity and NaOH concentration. Temperature shows a higher effect when compared with NaOH and retention time ((Figure 43). Thus, it can be inferred that NaOH loading can be reduced by increasing temperature. The predictive model (Equation 14) for arabinose release in the function of temperature and time of exposition to the hydrothermal pretreatment covered of the data obtained (R^2 of 94.63%).

$$\text{Arabinose}_{AB} = 0.72 + 0.14x_1 + 0.12x_2 + 0.06x_3 + 0.04x_1x_2 \qquad \textit{Equation 19}$$

Temperature effect on thermo chemically pretreated AB has been extensively studied. For instance, Arreola- Vargas *et al.,* (2015) explored the interactions of temperature (°C), HCl concentration (%w/v) and retention time (min) with sugars recovery from cooked and uncooked agave bagasse. Of these, temperature showed the strongest effect on sugar recovery. However, concentration of 5-HMF increased along with treatment severity. Aguirre-Fierro *et al.,* (2020) studied the effects of high pressure CO_2-H_2O, temperature and residence times on the AB by making use of a 3^2 factorial design. Similar to the present study, hemicellulose was more prone to hydrolysis than cellulose. Glucose concentration remained constant among the different conditions tested. Temperature and time were found to have a positive significant linear effect on the overall sugar yield.

2D and 3D response surface plots show the interactions for two independent variables while keeping the other variable at CP. Figure 21 shows the interactions of temperature (°C), NaOH (M) and retention time (min) on arabinose release from AB.

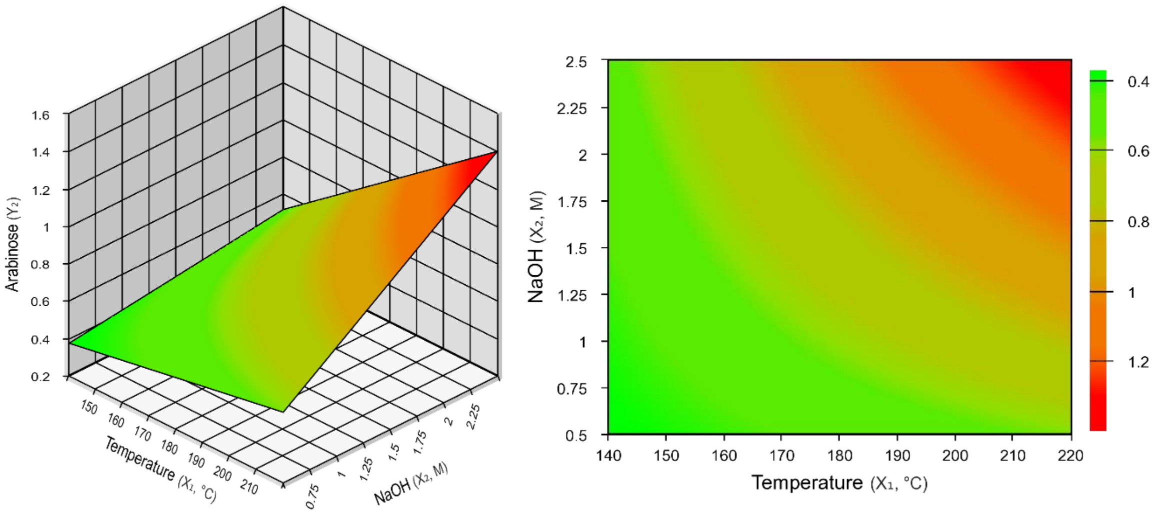

Figure 21 Response surface 3D and 2D plots indicating the effect of the interaction between: temperature and NaOH on arabinose release from agave bagasse (AB)

5.4.2 Effect on solid hydrolysate composition

Temperature (ºC) and NaOH concentration (M) had a significant (p-value <0.05) negative linear effect on solids recovery from AB (Figure 40). A model was predicted with CCRD (Equation 20) indicating the linear effect of temperature (ºC) and NaOH concentration (M) on solids recovery (%) from AB.

$$\text{Solids recovery}_{AB} = 30.34 - 6.84x_1 - 3.75x_2 \qquad \textit{Equation 20}$$

The coefficient of determination R^2 was used to test the accuracy of the model. A value of $R^2 = 80.22\%$ was found.

2D and 3D response surface plots (Figure 22) show the interactions of temperature (°C) and NaOH (M) on solids recovery from empty fruit bunch.

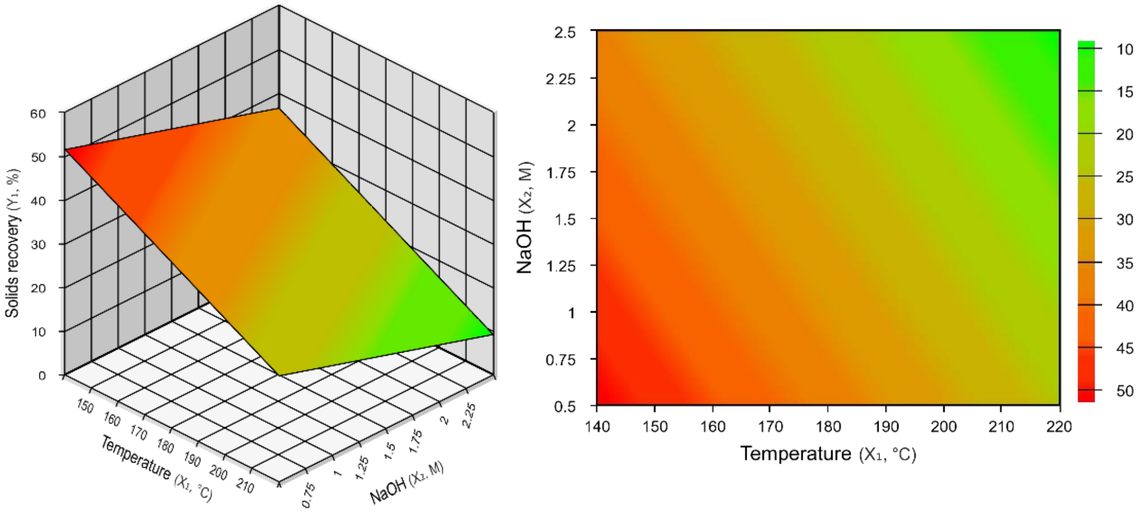

Figure 22 Response surface 3D and 2D plots indicating the effect of the interaction between x1: temperature (ºC) and x2: NaOH concentration (M) on solids recovery from agave bagasse (AB)

5.4.3 Effect on biomethane potential (BMP).

Manometric BMP test were carried out according to section 4.3.3. Table 8 shows the BMP potential of raw and treated AB. AHPT hydrolysates from the CP conditions (180°C, 1.5M NaOH, 20min) presented a higher methane production in both the mono and the co digestion trials. SH and LH monodigestion resulted in 286 and 302 ml CH_4 gVS^{-1}, respectively. This suggest that high cellulose exposure and high sugar recovery with low concentration of inhibitory compounds was achieved for SH and LH, respectively.

Table 8 Biomethane potential (BMP) of raw and alkaline hydrothermal pretreatment agave bagasse (AB) hydrolysates at central point (CP) conditions (180°C, 1.5M NaOH, 20min).

	BMP (ml CH_4 gVS^{-1})
Raw AB	150
CP co digestion hydrolysates	257
CP solid hydrolysate	286
CP liquid hydrolysate	302

RSM application to study the interactions between the operational variables an the BMP of AB was not possible due to C2, C3, C4, C11 and C12 presenting null production of methane. Therefore, the coupled effect of time and temperature referred as treatment severity and NaOH concentration interaction with BMP of AB can be only observed as a 2D interaction.

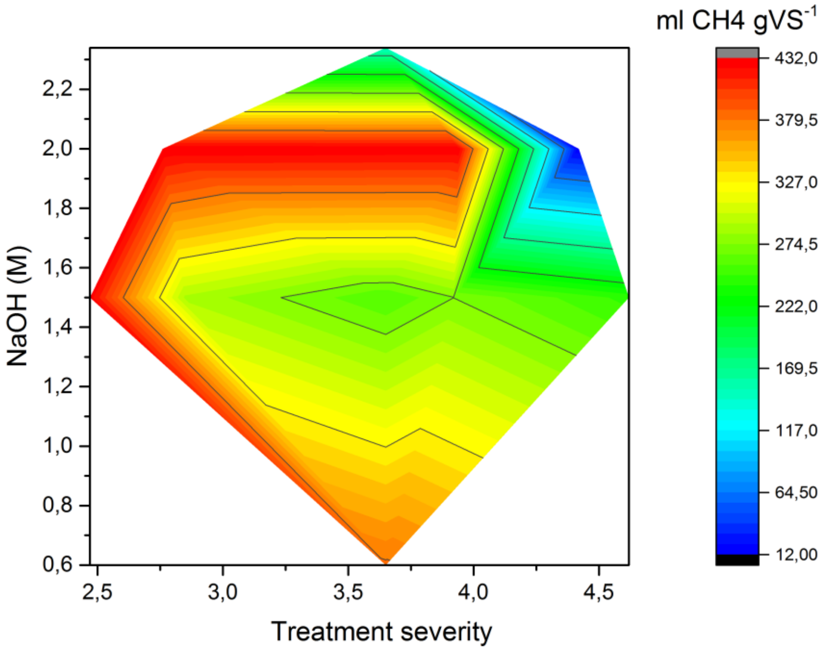

Figure 23 Biomethane potential from co digestion of alkaline hydrothermally pretreatment agave bagasse (AB) hydrolysates as a function of treatment severity and NaOH concentration

5.4.4 Effect on methane content in biogas

Figure 24 shows the effect of treatment severity and NaOH concentration (M) on methane content of biogas produced from the co digestion of agave bagasse alkaline hydrolysates.

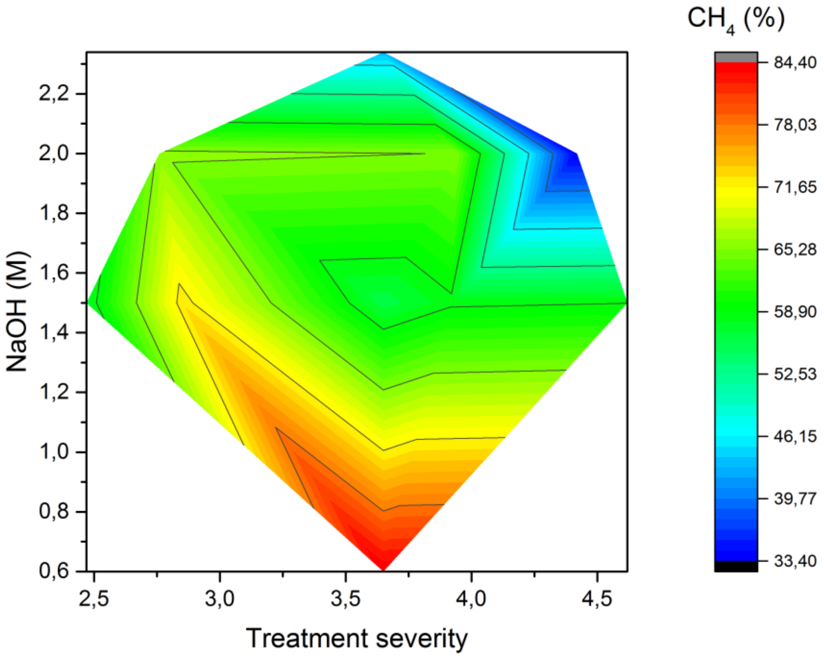

Figure 24 Methane content in biogas produced from co digestion of alkaline hydrothermally pretreatment agave bagasse (AB) hydrolysates as a function of treatment severity and NaOH concentration

5.5 Comparison among fibers

The effects of AHPT on sugars recovery, BMP and methane production were found to be fiber specific. Sugars recovery varied in concentration and composition for all fibers. A maximum sugar recovery of 4.69g L^{-1} was found for SCB followed by AB and EFB with a maximum total sugars concentration in the LH of 3.49g L^{-1} and 1.47g L^{-1}, respectively. Maximum recovery was achieved at 213°C, 1.5M NaOH and 20min of retention time for SCB and AB whereas for EFB mildest conditions (200°C, 2M NaOH, 10min) where needed to achieve the maximum sugars recovery. This suggest that cellulose and hemicellulose degradation increases at higher treatment severities for SCB and AB. However, at high treatment severities inhibitory degradation products can be formed resulting in lower bioenergy yields. Detrimental effects of inhibitory compounds are not restricted to their concentration in the hydrolysates but also their composition, the more types the higher inhibition (Rolly et al., 2016).

In terms of the composition of the liquid hydrolysate it was observed that glucose was the main sugar recovered for SCB and EFB this suggest that hemicellulose component could be formed by glucose as a branched polymer with substitutions of arabinose and xylose. Whereas hemicellulose degradation products (arabinose and xylose) were found in a higher proportion for AB. SCB and AB showed a linear interaction between the operational conditions and glucose release however, the maximum recovery conditions does not imply that there is a higher potential for bioenergy production processes since inhibitory compounds concentration could be high as well. The quadratic effect of temperature and time found for glucose release from EFB fibers suggest that there is a maximum glucose release at 180°C, 1.5M NaOH, and 20min retention time after which further degradation of glucose into inhibitory compounds starts to occur. Arabinose release presented a positive linear interaction with all the AHPT conditions.

Maximum solids recovery of 24%, 50% and 41% were achieved for SCB, EFB and AB, respectively. This gives a rough indication on the effect on AHPT on delignification and hemicellulose solubilization. At low solids recovery, enhanced delignification, increased sugars solubilization along with increased cellulose exposure can be expected.

The variable composition of AHPT hydrolysates could lead to different methane yields for each fiber and set of conditions. For instance, Asri & Afila (2018) found that even when two monosaccharides present the same chemical and molecular composition, their BMP is different since theoretical biogas potential equations such as the one presented by Buswell & Mueller (1952) do not consider the spatial arrangement of atoms in the sugar molecules nor the type intermediate products resulting from the substrate degradation in the anaerobic digestion stages. Therefore, biogas production from co digestion systems can be expected to vary according to the LH sugar matrix.

Low biogas yield was observed for the co digestion of SCB hydrolysates with a maximum production of 266ml CH_4 gVS^{-1} in comparison with 431 ml CH_4 gVS^{-1} for both EFB and AB. Decreased BMP for SCB can be explained by the high NaOH concentration (6.4 g L^{-1}) in the anaerobic reactor which was above the inhibitory values mentioned in literature.

Even though SCB, EFB and AB fall under the classification of agro industrial residues, they present structural and compositional variations (Table 5). Not only the concentration of the cellulose, hemicellulose and lignin play a role on LB bioenergy yields, the structure and individual characteristics of these components also influences their hydrolysis capacity. For instance, lignin is composed of p-hydroxyphenyl (H), guaiacyl (G) and syringyl (S) units; the ratio of these components varies according to the biomass type and it has affects the efficiency of AHPT. Shimizu et al. (2012) found that the higher the S/G are, the higher delignification of LB. The S/G for SCB, EFB and AB have been found to be 1.1, 2.86 and 4.3 for SCB, EFB and AB, respectively. However, lignin removal is not neccearly achieved at higher treatment severities since lignin can be redistributed in the fibers (Hendriks and Zeeman, 2009). Rolly et al., (2016) stated that the probability of cellulose and hemicellulose take up in bioenergy processes is affected by the interactions and modifications with the polymers that form lignin. Ferulic acid content in lignin as well as cellulose degree of polymerization have also been found to affect the AHPT carbohydrates hydrolysis capacity (Mittal et al. 2011; Wu et al., 2011). EFB has been found to have a higher crystallinity index (50%) in comparison with AB (27%) which can be attributed to the presence of agave´s pulp in the residual bagasse.

5.6 Energy gain from lignocellulosic biomass alkaline hydrothermal pretreatment.

Energy requirements alkaline hydrothermal pretreatment.

The net energy gain for the CCRD conditions of the three fibers was analyzed. Results are shown in Table 9. The energy gain was calculated subtracting the amount of energy required to maintain the hydrothermal pretreatment from the energy surplus of co digestion of fiber´s hydrolysates compared to that of raw fiber.

Co digestion of sugarcane bagasse did not present energy gains at any of the CCRD conditions tested. This is related with the low BMP of the co digestion runs as well as the low solids recovery yield for these fibers. Conditions 1, 3,6,13, and the central point of EFB co digestion lead to positive net energy gains. These conditions include –α and -1 values for the independent variables. Therefore, they presented a synergy between solids recovery (%), BMP and low energy requirements for the hydrothermal pretreatment. Condition 1 gave the highest energy gain with 3.53MJ Kg^{-1} treated EFB. In the case of AB, conditions 3, 11 and 13 presented a positive energy gain. Of these, condition 13 which correspond to –α values for temperature (°C) gave the maximum energy gain with 4.77MJ Kg^{-1} treated AB.

Table 9 Energy gain from anaerobic co digestion of SCB, EFB and AB alkaline hydrolysates. C1 (146ºC, 1.5M, 20 minutes), C2 (160 ºC, 1M, 10 minutes), C3 (160 ºC, 2M, 30 minutes), C4 (160ºC, 1M, 30 minutes), C5 (160ºC, 2M, 10 minutes), C6 (180 ºC, 0.66M, 20 minutes) C7 (180 ºC, 1.5M, 3.18 minutes), C8 (180 ºC, 1.5 M, 36.82 minutes), C9 (200 ºC, 2.34M, 20 minutes), C10 (200 ºC, 2M, 30 minutes), C11 (200 ºC, 1M, 30 minutes), C12 (200 ºC, 1M, 10 minutes), C13 (200 ºC, 2M, 10 minutes), C14 (213.64 ºC, 1.5M, 20 minutes), CP (180 ºC, 1.5M, 20 minutes)

	Energy hydrothermal process (MJ Kg^{-1} Treated fiber			**BMP (MJ Kg^{-1} Treated fiber)**			**Net energy gain (MJ Kg^{-1} Treated fiber)**		
	SCB	**EFB**	**AB**	**SCB**	**EFB**	**AB**	**SCB**	**EFB**	**AB**
C1	5.4	5.4	5.4	2.2	12.7	15.4	-7.0	1.2	4.8
C2	6.1	6.0	6.0	4.3	15.7	ND	-5.4	3.5	ND
C3	6.1	6.0	6.0	4.5	9.2	ND	-5.3	-3.0	ND
C4	6.1	6.0	6.0	1.1	10.5	ND	-8.7	-1.7	ND
C5	6.1	6.0	6.0	2.0	12.5	14.9	-7.7	0.3	3.6
C6	7.0	6.9	7.0	1.0	10.3	11.6	-9.7	-2.9	-0.6
C7	7.0	6.9	7.0	0.1	14.3	10.5	-10.6	1.1	-1.7
C8	7.0	6.9	7.0	1.5	11.2	9.1	-9.2	-1.9	-3.1
C9	7.0	6.9	7.0	7.0	4.7	5.5	-3.7	-8.4	-6.8
C10	8.0	7.9	7.9	3.5	10.1	ND	-8.2	-4.1	ND
C11	8.0	7.9	7.9	2.8	9.9	ND	-8.9	-4.2	ND
C12	8.0	7.9	7.9	2.4	6.6	ND	-9.2	-7.6	ND
C13	8.0	7.9	7.9	6.1	7.2	16.3	-5.6	-6.9	3.1
C14	8.7	8.6	8.6	2.2	5.7	6.7	-10.2	-9.1	-7.2
CP	7.0	6.9	7.0	3.8	13.4	8.3	-6.9	0.3	-4.0

AHPT improves the methane content and BMP of LB. However, high costs associated with chemical consumption (NaOH) decrease the feasibility of application of this treatment. Table 10 shows the energy requirements and associated cost for NaOH usage in the pretreatment of lignocellulosic biomass. If the energy required for NaOH production were to be included in the calculations for section 5.6 the net energy gain at for SCB, EFB and, AB at all conditions would be negative.

Table 10 Cost and energy requirements attributed to NaOH consumption at different operational conditions for lignocellulosic biomass treatment at a solid to liquid ratio of 1:10.

	Kg NaOH Kg^{-1} raw dry fiber	Cost ($)	Energy (MJ)
0.66	0.3	0.1	4.8
1	0.4	0.2	7.2
1.5	0.6	0.3	10.8
2	0.8	0.4	14.4
2.34	0.9	0.4	16.8

Since NaOH production is a high energy intensive process, the exploration of NaOH recovery routes needs to be carried out.

5.7 Theoretical estimation for NaOH recovery

As it could observed from previous sections, the amount of biogas produced as well as its composition depend on the substrate characteristics. The theoretical estimation of the amount of energy needed for NaOH recovery from an AD system treating 1 ton of lignocellulosic waste was calculated. The calculation was divided in 4 stages. First, the theoretical amount of biogas produced by the lignocellulosic waste and its composition was calculated, in this stage the lignocellulosic waste is assumed to be a carbohydrate rich substrate. Second, this the amount of NaOH needed CO2 removal for biogas upgrading to 90% on methane was calculated. Third, the amount of NaHCO3 generated by CO2 solubilization with the NaOH solution this is, the amount of NaHCO3 present in the digestate was calculated. Finally, the amount of energy needed for NaOH recovery from the digestate was estimated.

According to Buswell & Mueller (1952), the theoretical composition of biogas from a certain substrate can be calculated as follows:

$$C_xH_yO_z + \left(x - \frac{y}{4} - \frac{z}{2}\right)H_2O \rightarrow \left(\frac{x}{2} + \frac{y}{8} - \frac{z}{4}\right)CH_4 + \left(\frac{x}{2} - \frac{y}{8} + \frac{z}{4}\right)CO_2$$

Lignocellulosic biomass is mainly conformed of cellulose and hemicellulose which are degraded into hexoses $C_6H_{12}O_6$, and pentoses $C_5H_{10}O_5$, respectively. The theoretical biomass composition for both carbohydrates is the same; 50% of CH_4 and 50% of CO_2. Further calculations considered lignocellulosic biomass as a glucose substrate.

From 1ton of lignocellulosic waste, 33,304.4mol of biogas, with a composition of 50% CH_4 and 50% CO_2, are produced. Biogas composition affects its energy content; methane has a calorific value of 10KWh m^{-3} the presence of CO_2 decreases the energy content of the biogas since it is non-combustible (Kapoor *et al.,* 2019). Thus, lignocellulosic waste biogas has a calorific value of 5KWh m^{-3}. Biogas use in energy production systems is hindered by its composition; CO_2 results in storage and transportation complications (Kapoor *et al.*, 2019).

In order to upgrade the biogas to a 90% CH_4 content, 14,801.87 mols of CO_2 need to be removed. In this study removal of CO_2 with NaOH was explored in order to have a rough comparison with the in situ biogas upgrading achieved by the co digestion of the hydrolysates obtained from AHPT of SCB, EFB and AB.

The removal of CO_2 using a NaOH solution is carried out with the next reactions:

R1: $2NaOH_{(aq)} + CO_{2\,(g)} \rightarrow Na_2CO_{3\ (aq)} + H_2O_{(l)}$

R2: $Na_2CO_{3\ (aq)} + H_2O_{(l)} + CO_{2\,(g)} \rightarrow 2NaHCO_{3\ (aq)}$

R3: $NaOH_{(aq)} + CO_{2\,(g)} \rightarrow NaHCO_{3\ (aq)}$ with $\Delta H°_{298K} = -131.5KJ$

Where $\Delta H°_{298K}$ is the amount of energy consumed (+) or produced (-) per mol in a reaction.

Biogas upgrading is an energy intensive process due to the high amount of energy required in NaOH production. According to Brinkmann *et al.,* (2014) 5KWh of primary energy are required per Kg of NaOH produced with Chlor-alkali systems. Therefore, the evaluation of NaOH recovery from the $NaHCO_3$ rich digestate, as a means to increase the net energy gains from co digestion of AHPT hydrolysates is of importance. Nikulshina *et* *al.*, (2008) showed the equilibrium composition for $NaHCO_3$ and air containing CO_2 (Figure 25). By increasing the temperature, the equilibrium starts to shift and different Na species are found.

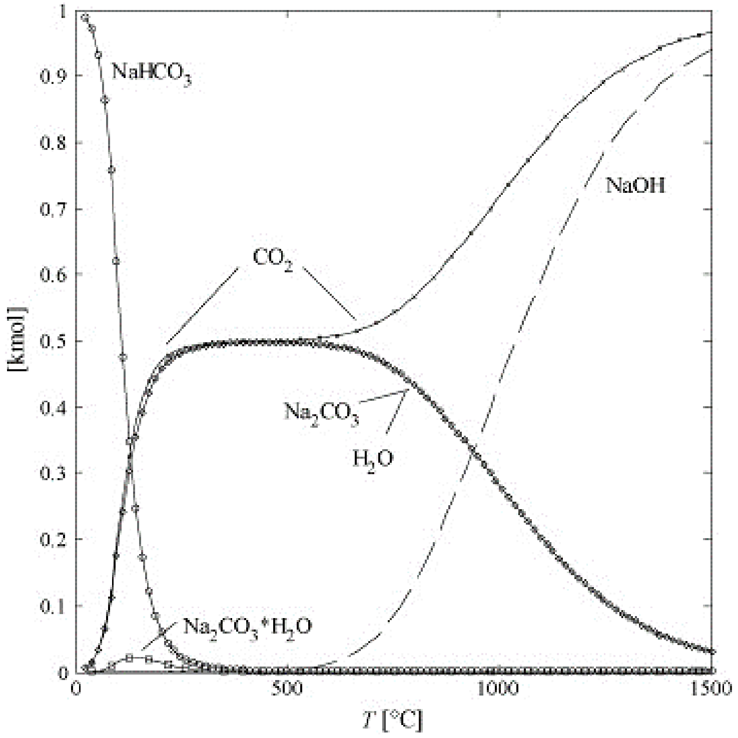

Figure 25 Equilibrium composition of 1 kmol NaHCO3 (s) vs. temperature at 1 bar. Taken from Nikulshina et al., (2008)

It can be observed (Figure 25) that $NaHCO_3$ can be thermally decomposed into NaOH. According to Nikulshina *et al.*, (2008), this process consists of the next stages:

1. Around 80°C reaction 2 is reversed and thermal decomposition of $NaHCO_3$ starts to occur. Above 312°C Na_2CO_3 is the only Na based compound in equilibrium.

R4: $2NaHCO_{3\,(aq)} \rightarrow Na_2CO_{3\,(aq)} + H_2O_{(l)} + CO_{2\,(g)}$ with $\Delta H°_{298K} = +135.5KJ$

2. If the solution continues to be heated up, Na_2CO_3 in the presence of water vapor will start to hydrolyze into Na_2O. The reaction is completed around 1500°C where only Na_2O is present.

R5: $Na_2CO_{3\,(aq)} \rightarrow Na_2O + CO_2$ with $\Delta H°_{298K} = 720.7KJ$

3. Lastly, Na_2O reacts with H_2O at 727°C to produce $NaOH$.

R6: $Na_2O + H_20 \rightarrow 2NaOH$ with $\Delta H°_{298K} = -541.3KJ$

According to $\Delta H°_{298K}$ of reactions R4 to R6 158KJ are needed to recover 1mol of NaOH from 1 mol of $NaHCO_3$ present in the digestate. Therefore, the amount of energy needed to recover NaOH from LB digestate is 2.3GJ. The energy needed for the thermal degradation of $NaHCO_3$ into NaOH could be provided by sunlight uptake energy producing systems since SCB, EFB and AB are produced in countries with high direct incoming solar radiation. Concentrated solar power (CSP) has been gaining attention for energy saving purposes. For instance, McGregor (2019) implemented a CSP system equipped with Fresnel lenses in the hydrothermal pretreatment of EFB. The system reached temperatures as high as 400°C in only a matter of seconds and contributed to an increase in the BMP of EFB from 132 ml CH_4 gVS^{-1} to 268 ml CH_4 gVS^{-1}. McGregor (2019) made direct use of the CSP system for the pretreatment however, some studies have evaluated the feasibility of the CSP coupled with a cogeneration plant (CG) in order to minimize costs (El handami *et al.,* 2020). Likewise, CSP-CG systems allow the continuity of energy intensive processes since an integration with thermal energy storage technologies can be applied (Mohammadi & Khorasanizadeh, 2019).

Following findings by Islam *et al.,* (2019), an area of $8m^2$ of linear Fresnel lens is needed to produce 1MWh of electric energy considering a 21% of solar efficiency and a solar to electric energy conversion efficiency of 8 to 10%. This applies for sites with an annual average direct normal irradiance >1800KWh m^{-2}. Figure 26 show that Brazil, and Mexico fall under this category. Therefore, an area of $0.63m^2$ of concentrated solar power system equipped with Fresnel lenses is needed per ton of lignocellulosic waste fed to the anaerobic digesters.

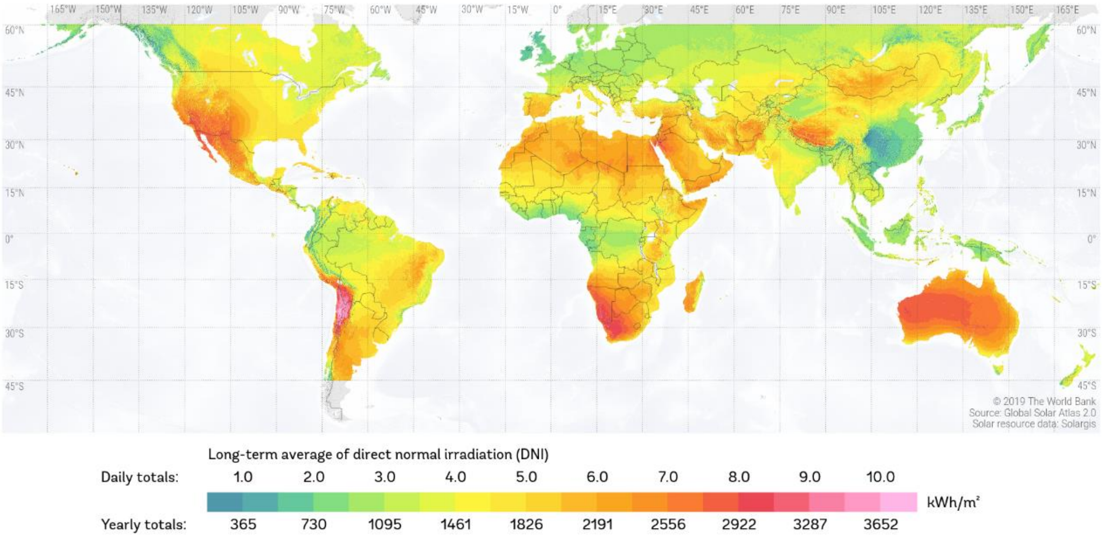

Figure 26 Average daily an annual direct normal irradiance (DNI) per country retrieved from https://solargis.com/maps-and-gis-data/download/world

6. CONCLUSIONS

The effect of alkaline hydrothermal pretreatment (AHPT) on the recalcitrance and biomethane potential (BMP) from sugarcane bagasse (SCB), empty fruit bunch (EFB) and agave bagasse (AB) was evaluated in this study. The effects of AHPT were found to be fiber specific. Additionally, biomass recalcitrance and methane production changed along the different temperature (°C), NaOH concentration (M), and residence time (min) conditions tested following a central composite rotatable design (CCRD) approach. Specific conclusions for the main research questions posed at the beginning of this work are presented below.

- What is the effect of AHPT on LB recalcitrant characteristics and sugars availability?

  Glucose release reached maximum concentration of 4mg L^{-1}, 0.8mg L^{-1} and 1.5 mg L^{-1} for SCB, EFB and AB, respectively. Glucose release presented a significant (p-value <0.05) linear positive interaction with temperature and retention time for SCB and AB fibers. A significant (p-value <0.05) quadratic interaction of temperature and retention time was found for EFB. Maximum arabinose concentrations from SCB, EFB and AB were 0.7mg L^{-1}, 0.7mg L^{-1}, and 1mg L^{-1}, respectively. Arabinose release presented a significant (p-value <0.05) positive linear interaction with temperature and NaOH concentration for SCB and EFB fibers. Whereas a significant (p-value <0.05) positive linear interaction with temperature, NaOH concentration and retention time was observed for AB fibers. Lignin content in SCB fibers presented a significant (p-value <0.05) interaction with the coupled effect of temperature and NaOH concentration. Temperature and NaOH had a significant (p-value <0.05) negative linear effect with fiber recovery. The variations in the effects on the recalcitrance of the fibers can be attributed to the different compositional, structural characteristics of the fibers.

- What is the effect of AHPT on LB biogas yield and biogas composition through thermophilic anaerobic digestion?

  BMP from fibers pretreated at 180°C, 1.5M NaOH and 20min was found to be fiber specific. BMP for treated SCB was increased from 112 ml CH_4 gVS^{-1} to 318ml CH_4 gVS^{-1} in comparison with for raw fiber. Treated EFB presented a lower (195 ml CH_4 gVS^{-1}) BMP than the raw fiber (113 ml CH_4 gVS^{-1}) possibly related with the presence of anaerobic digestion inhibitory compounds. Likewise, a low (44ml CH_4 gVS^{-1}) BMP for liquid SCB hydrolysate was found. This can be attributed to a high Na^+ concentration in the anaerobic digester.

Raw and treated fiber presented the same methane content in the biogas with 40% CH_4 for SCB and EFB and 50% CH_4 for AB. Whereas, methane content in SCB, EFB and AB liquid hydrolysates was increased to 55% CH_4, 65% CH_4 and 60% CH_4, respectively probably due to the interactions between the carbonate species and NaOH present in the liquid hydrolysate.

- Does co-digestion of solid and liquid hydrolysates from AHPT of LB contribute to in-situ biogas upgrading through CO_2 solubilisation? If so, to what extent?

  Co digestion of liquid and solid hydrolysates obtained from SCB, EFB and AB undergoing AHPT derived in biogas with a higher methane composition. NaOH concentration presented a significant ($p\text{-value} < 0.05$) positive linear and quadratic interaction with methane content in SCB and EFB hydrolysates, respectively. No specific conclusions can be drawn for NaOH effect on methane content of AB hydrolysates due to experimental errors. However, it was observed that low NaOH coupled with low treatment severities contribute to an increase in methane content.

- Does NaOH regeneration contribute to energy savings in the AHPT of LB?

  NaOH regeneration could contribute to an increase in net energy gain from AHPT by decreasing the energy consumption attributed to NaOH consumption in AHPT.

- Further remarks.

  The optimal operational conditions considering the amount of energy spent on the heat requirements of the hydrothermal reactor were different to those were only biogas production is considered. Net energy gain depends not only on biogas production but also on the amount volatile solids recovered from the dry fiber as liquid and solid hydrolysates volatile solids. No energy gain was observed for SCB undergoing AHPT. Maximum energy gain of 3.53MJ $Kg^{-1}$for EFB pretreated at 160°C, 1M NaOH and 10min retention time was observed. AB presented a maximum energy gain of 4.77MJ Kg^{-1} when pretreated at 146°C, 1.5M NaOH and 20min retention time.

7. RECOMMENDATIONS

The high variability on the response variables among the different treatment conditions and fibers of interest exhibit the need for a thorough evaluation of the lignocellulosic biomass structural and compositional characteristics and their influence on bioenergy productions processes. Effects of AHPT on inhibitory compounds formation, cellulose crystallinity and delignification must be evaluated and considered as response variables for all fibers of interest in order deepen the understanding of the solid and liquid hydrolysates contribution to BMP. Moreover, net energy gains from AHPT need to evaluated and considered as response variables.

Energy saving scenarios such as increase in the fiber to dilute NaOH ratio to decrease the energy expenditure in the hydrothermal reactor and practical thermal recovery of NaOH from the digestate could be implemented. Furthermore, practical evaluation on the energy generation capacity of a concentrated solar power system and its efficiency for conversion into electrical energy needs to be carried out. The preceding could help to assess the extent to which bioenergy productions systems using LB as feedstock can be sustained by means of renewable energy.

Advantages of LB AHPT need to be evaluated by carrying out a techno economic analysis. Factors such as the energy and chemicals expenditure in the pretreatment and anaerobic digestion stages influence the feasibility of the processes. If one were to carry out a techno economic analysis pilot or full scale plants would provide a better indication of the advantages of lignocellulosic biomass pretreatment. Lab scale batch assays give only a general overview on the BMP capacity of lignocellulosic biomass hydrolysates. Batch anaerobic digestion is less susceptible to inhibition since the activity of the inoculum is high contrary to continuous operation where the concentration of inhibitory compounds increases with each feeding since their degradation rate is low to none. Furthermore, a continuous system would allow the evaluation of the seasonal variations of lignocellulosic biomass effects on biogas yield. If the feasibility for biogas production from LB is found to be low, alternative approaches such as biorefinery systems can be evaluated.

8. ACKNOWLEDGEMENTS

The author would like to express gratitude towards the Secretary of Energy (SENER) from Mexico for granting financial support for the master studies through the National Council on Science and Technology (CONACYT) with the CONACYT-SENER energetic sustainability scholarship.

9. REFERENCES

Aguirre-Fierro A., Ruíz H.A., Cerqueira, M.A., Ramos-González R., Rodríguez-Jasso R.M., Marques S., & Lukasik R.M. (2020). Sustainable approach of high-pressure agave bagasse pretreatment for ethanol production. *Renewable Energy, 155*: 1347-1354.

Antonopoulou, G. & Lyberatos, Gerasimos. (2012). Effect of Pretreatment of Sweet Sorghum Biomass on Methane Generation. *Waste and Biomass Valorization*.

Arreola-Vargas J., Ojeda-Castillo V., Snell-Castro R., Corona-González RI., Alatriste-Mondragón F., Méndez-Acosta HO. (2015). Methane production from acid hydrolysates of Agave tequilana bagasse: evaluation of hydrolysis conditions and methane yield. *Bioresource Technoogy*, *181*:191-199.

Asri, O., & Afilal, M. E. (2018). Comparison of the experimental and theoretical production of biogas by monosaccharides, disaccharides, and amino acids. *International journal of environmental science and technology*, *15:* 1957-1966.

Bajpai, P. (2017). Basics of Anaerobic Digestion Process. *Anaerobic Technology in Pulp and Paper Industry*, 7–13.

BP (2019). Energy Outlook

Buffiere, P., Loisel, D., Bernet, N., & Delgenes, J.-P., (2006). Towards New Indicators Forthe Prediction of Solid Waste Anaerobic Digestion Properties. *Water Science Technology*, *53*:233–241.

Buswell, A. M., & Mueller, H. F. (1952). Mechanism of Methane Fermentation. *Industrial & Engineering Chemistry*, *44(3)*, 550–552.

Caldarelli C., Moraes M., Paschoalino P. (2017). Sugarcane industry effects on the GDP per capita in the Center-South region of Brazil. *Revista de Economia e Agronegócio - REA*, *15*: 183–200.

Carrere H, Antonopoulou G, Affes R, et al. (2016). Review of feedstock pretreatment strategies for improved anaerobic digestion: From lab-scale research to full-scale application. *Bioresource Technoogy, 199*:386-397. doi:10.1016/j.biortech.2015.09.007

Carrillo-Nieves D., Rostro M., de la Cruz R., Ruíz H., Iqbal H., & Parra-Saldivar R. (2019). Current status and future trends of bioethanol production from agro-industrial wastes in Mexico. *Renewable and Sustainable Energy Reviews*, *102*: 63-74

Chang V.S. & Holtzapple, M.T. (2000) Fundamental Factors Affecting Biomass Enzymatic reactivity, *Applied Biochemistry and Biotechnology*, *84*:5–37

Consejo Regulador del Tequila, CRT. URL: https://www.crt.org.mx/EstadisticasCRTweb/. Accessed 08 Sep 2019

Costa A., Pinheiro G., Pinheiro F., dos Santos A., Santaella S., & Leitão R. (2014). The use of thermochemical pretreatments to improve the anaerobic biodegradability and biochemical methane potential of the sugarcane bagasse. *Chemical Engineering Journal, 248*: 363-372

De Moraes G., Marcos V., Gonçalves A., Fernandes V., Martín C. (2015). Influence of mixed sugarcane bagasse samples evaluated by elemental and physical–chemical composition. *Industrial Crops and Products, 64*: 52-58

Egal, M.; Budtova, T.; Navard, P. (2007). Structure of aqueous solutions of microcrystalline cellulose/sodium hydroxide below 0 degrees C and the limit of cellulose dissolution. *Biomacromolecules, 8 (7):*2282−7.

El hamdani F., Abderafi S., Vaudreuil S., BounahmidiT. (2020). Techno-Economic Evaluation of a CSP Plant Driven by an Organic Rankine Cycle. *Journal of Solar Energy Engineering*. 1-36.

Fan, S., Zhang, P., Li, Fan. Jin, S., Wang, S., & Zhou, S. (2016). A review of lignocellulose change during hydrothermal pretreatment for bioenergy production. *Current Organic Chemistry*. 20: 2799-2809

Ge X, Xu F, Li Y. (2016). Solid-state anaerobic digestion of lignocellulosic biomass: Recent progress and perspectives. *Bioresource Technol*ology, *205*:239-249.

Gebreeyessus GD & Jenicek P. (2016). Thermophilic versus mesophilic anaerobic digestion of sewage sludge: a comparative review. *Bioengineering, 14:* 1-14.

Giele D., Boshell F., Saygin D., Bazilian M., Wagner N. & Gorini R. (2019). The role of renewable energy in the global energy transformation. *Energy Strategy Reviews, 24*:38-50.

Gielen D., Boshell F., Saygin D., Bazilian M., Wagner N., & Gorini R. (2019). The role of renewable energy in the global energy transformation. *Energy Strategy Reviews, 24:* 38-50.

Gonzales, R. R., Sivagurunathan, P., & Kim, S. H. (2016). Effect of severity on dilute acid pretreatment of lignocellulosic biomass and the following hydrogen fermentation. *International Journal of Hydrogen Energy, 41*(46): 21678-21684.

González M., Ohra-aho T., Tamminen T., daSilva D., Campargue M., Dupont C. (2019). Detailed structural elucidation of different lignocellulosic biomass types using optimized temperature and time profiles in fractionated Py-GC/MS. *Journal of Analytical and Applied Pyrolysis, 140*:112-124

González, M.R.C., Crespo González, M.R., González Eguiarteq, D.R., Macías, R.R., Salcido, L.A.R., Del Real Laborde, J.I., Morán, J.P.T. (2018) Evaluation of agave bagasse compost as a substrate component to produce tequila blue agave seedlings. *Mexican Journal Agricultural Science, 4:*1161–1173.

Han, Minhee & Kim, Yule & Kim, Seung & Choi, Gi-Wook. (2011). High efficiency bioethanol production from OPEFB using pilot pretreatment reactor. *Journal of Chemical Technology and Biotechnology,* 86:1527 - 1534. 10.1002/jctb.2668.

He, L., Huang H., Zhang Z., Lei, Z. (2015). A Review of Hydrothermal Pretreatment of Lignocellulosic Biomass for Enhanced Biogas Production. *Current Organic Chemistry, 19:* 437-446.

Hong, J.Y., Kim, Y.S., & Oh, K.K. (2013). Fractionation and delignification of empty fruit bunches with low reaction severity for high sugar recovery. *Bioresource technology, 146*, 176-183.

Hosseini SE, Abdul Wahid M. (2015). Pollutant in palm oil production process. *Journal of the Air and Waste Management Association,65(7):*773-781.

IEA. (2020). An Introduction To Biogas And Biomethane – Outlook For Biogas And Biomethane: Prospects For Organic Growth Analysis. Retrieved from: https://www.iea.org/reports/outlook-for-biogas-and-biomethane-prospects-for-organic-growth/an-introduction-to-biogas-and-biomethane

Intergovernmental Panel on Climate Change (IPCC), Climate Change 2014: Synthesis Report. Contribution of Working Groups I, II, and III to the Fifth Assessment Report of the Intergovernmental Panel on Climate Change, IPCC, Geneva, 2014

International energy agency. (2017). World Energy Outlook.

IRENA (2018), *Global Energy Transformation: A roadmap to 2050*, International Renewable Energy Agency, Abu Dhabi.

Islam Md., Tasbirul H., Nazmul SR. (2019). Current energy mix and techno-economic analysis of concentrating solar power (CSP) technologies in Malaysia. *Renewable Energy, Elsevier, 140(C):*789-806.

Jönsson LJ., Martín C. (2016). Pretreatment of lignocellulose: Formation of inhibitory by-products and strategies for minimizing their effects. *Bioresource Technology,*199:103-112.

Kapoor R., Ghosh P., Kumar M., Vijay VK. (2019). Evaluation of biogas upgrading technologies and future perspectives: a review. *Environmental Science and Pollution Research, 26 (12):*11631-11661

Karimi K., Shafiei M., Kumar R. (2013). Progress in physical and chemical pretreatment of lignocellulosic biomass. *Biofuel Technologies.*

Kim S. (2018). Enhancing Bioethanol Productivity Using Alkali-Pretreated Empty Palm Fruit Bunch Fiber Hydrolysate. *BioMed Research International*.

Kumari S., & Das D. (2014). Improvement of gaseous energy recovery from sugarcane bagasse by two stage biohythane production. *Bioresurce Technology,* 194:354-363.

Lam S., Tsang Y., Yuh P., Keey R., Shahril M., Peng W., Lee W., Park Y. (2019). Co-processing of oil palm waste and waste oil via microwave co-torrefaction: A waste reduction approach for producing solid fuel product with improved properties. *Process Safety and Environmental Protection 128*:30-35.

Li, Renfei & Tan, Wenbing & Zhao, Xinyu & Dang, Qiu-Ling & Song, Qidao & Xi, Beidou & Zhang, Xiaohui. (2019). Evaluation on the Methane Production Potential of Wood Waste Pretreated with NaOH and Co-Digested with Pig Manure. *Catalysts*.

Lobo-Baêta BE., Lima DR, Adarme OF., Gurgel LV., Aquino SF. (2016). Optimization of sugarcane bagasse autohydrolysis for methane production from hemicellulose hydrolyzates in a biorefinery concept. *Bioresource Technology,200:*137-146.

Lopes E., Carraro A., Fernandes F., Rabelo K., Jesus G. & Honor A. (2019). Central composite rotatable design for startup optimization of anaerobic sequencing batch reactor treating biodiesel production wastewater. *Journal of Environmental Chemical Engineering, 7.*

Ma, Shuaishuai & Wang, Hongliang & Li, Jingxue & Fu, Yu & Zhu, Wanbin. (2019). Methane production performances of different compositions in lignocellulosic biomass through anaerobic digestion. *Energy, 189.*

Mancini G., Papirio S., Lens P., & Esposito G. (2016). Solvent Pretreatments of Lignocellulosic Materials to Enhance Biogas Production: A Review. *Energy Fuels, 30:* 1892-1903.

Mao C., Yongzhong F., Xiaojiao W., Guangxin R. (2015). Review on research achievements of biogas from anaerobic digestion. *Renewable and Sustainable Energy Reviews, 45:* 540-555

McGregor J. (2019). In search of sun: Solar pretreatment to enhance biomethane potential of empty fruit bunch (EFB) fibers. Delft University of Technology, Delft, The Netherlands.

Mirahmadi, K., Mohseni Kabir, M., Jeihanipour, A., Karimi, K., & Taherzadeh, M. (2010). Alkaline Pretreatment of Spruce and Birch to Improve Bioethanol and Biogas Production. *Bio Resources, 5(2):*928-938.

Mittal, A, Katahira, R, Himmel, ME and Johnson, DK (2011). Effects of alkaline or liquid-ammonia treatment on crystalline cellulose: changes in crystalline structure and effects on enzymatic digestibility. *Biotechnology for Biofuels 4:* 16.

Modenbach A. (2013). Sodium hydroxide pretreatment of corn stover and subsequent enzymatic hydrolysis: An investigation of yields, kinetic modeling and glucose recovery. *Theses and Dissertations--Biosystems and Agricultural Engineering*. 17.

Mohammadi K., Khorasanizadeh H. (2019). The potential and deployment viability of concentrated solar power (CSP) in Iran. *Energy Strategy Reviews,* 24:358-369.

Mosier N., Wyman C,. Dale B., et al. (2005). Features of promising technologies for pretreatment of lignocellulosic biomass. *Bioresource Technology, 96(6)*:673-686.

Mustafa, A. M., Li, H., Radwan, A. A., Sheng, K., & Chen, X. (2018). Effect of Hydrothermal and Ca (OH) 2 Pretreatments on Anaerobic Digestion of Sugarcane Bagasse for Biogas Production. *Bioresource Technology, 259*:54–60.

Nanda, S., Azargohar, R., Dalai, A., Kozinski, J. (2015). An assessment on the sustainability of lignocellulosic biomass for biorefining. *Renewable and Sustainable Energy Reviews, 50*:925-941

Nikulshina, V. & Ayesa, N. & Galvez, Maria & Steinfeld, A. (2008). Feasibility of Na-based thermochemical cycles for the capture of CO2 from air- Thermodynamic and thermogravimetric analyses. *Chemical Engineering Journal, 140*: 62-70.

Noman M.T., Ashraf M.A., Jamshaid H., Ali A., (2018). A Novel Green Stabilization of TiO2 Nanoparticles onto Cotton, Fiber. Polym., 19:2268-2277.

Nunes A., Etchelet M., Ferreira A., Clavijo L., Loaces I., Noya F. & Etchebehere C. (2020). Alkaline pretreatment of yerba mate (Ilex paraguariensis) waste for unlocking low-cost cellulosic biofuel. *Fuel,* 226

Nunes A., Etchelet M., FerreiraA., Braga M., Clavijo L., Loaces I., Noya F., & Etchebehere C. (2020). Alkaline pretreatment of yerba mate (Ilex paraguariensis) waste for unlocking low-cost cellulosic biofuel. *Fuel.*

O-Thong S, Boe K, & Angelidaki I. (2012). Thermophilic Anaerobic Co-Digestion of Oil Palm Empty Fruit Bunches with Palm Oil Mill Effluent for Efficient Biogas Production. *Applied Energy, 93*:648-654.

Palomo, R., López, I., Islas, F., Galindo, K., Munguía, D., Rincón, J., Corté, M., Alatriste, F., & Razo, E. (2018). Agave Bagasse Biorefinery : Processing and Perspectives. *Clean technologies and Environmental Policy,* 1423–1441.

Patel A., Arora N., Sartaj K., Pruthi V., Pruthi P. (2016). Sustainable biodiesel production from oleaginous yeasts utilizing hydrolysates of various non-edible lignocellulosic biomasses. *Renewable and Sustainable Energy Reviews, 62:*836-855.

Paul, Subhash & Dutta, Animesh. (2018). Challenges and opportunities of lignocellulosic biomass for anaerobic digestion. *Resources, Conservation and Recycling, 130*: 164-174.

Perdana, A. F. P., Rahman, A. A., Sadrina, I. N., & Gozan, M. (2019). Optimization of pretreatment conditions for microwave-assisted alkaline delignification of empty fruit bunch by response surface methodology. *International Journal of Technology*, *10*(8): 1479-1487. https://doi.org/10.14716/ijtech.v10i8.3431

Phitsuwan P., Sakka K., & Ratanakhanokchai K. (2016). Structural changes and enzymatic response of Napier grass (Pennisetum purpureum) stem induced by alkaline pretreatment. *Bioresource Technology, 218*: 247-256.

Phitsuwan P., Sakka K. & Ratanakhanokchai K. (2016) Structural changes and enzymatic response of Napier grass (*Pennisetum purpureum*) stem induced by alkaline pretreatment. *Bioresource Technology, 218*:247-256

Phuttaro C., Sawatdeenarunat C., Surendra K., Boonsawang P., Chaiprapat S., Kumar S. (2019). Anaerobic digestion of hydrothermally-pretreated lignocellulosic biomass: Influence of pretreatment temperatures, inhibitors and soluble organics on methane yield. *Bioresource Technology, 284:*128-138.

Pol E, Bakker R, van Zeeland A, Sanchez Garcia D, Punt A, Eggink G. (2015). Analysis of by-product formation and sugar monomerization in sugarcane bagasse pretreated at pilot plant scale: differences between autohydrolysis, alkaline and acid pretreatment. *Bioresour Technology*, *181*:114-123. doi:10.1016/j.biortech.01.033.

Prakash J., Vigna C., Priya B., Abdullah N., Ponmurugan K., Blessing J. (2016). Modeling of polysaccharide extraction from Gossypium arboreum L. seed using central composite rotatable design. *International Journal of Biological Macromolecules, 86*:857-864.

Ren, N., Wang, A., Cao, G., Xu, J., Gao, L. (2009) Bioconversion of Lignocellulosic Biomass to Hydrogen: Potential and Challenges. *Biotechnology Advances, 27*:1051-1060.

Rios-gonzález, L. J., Morales-martínez, T. K., Rodríguez-flores, M. F., Rodríguez-de, J. A., Castillo-quiroz, D., Castro-montoya, A. J., & Martinez, A. (2017). Autohydrolysis pretreatment assessment in ethanol production from agave bagasse. *Bioresource Technology 242*: 184–190.

Robles E., Fernández J., Barbosa A., Gordobil O., Carreño N., Labidi J. (2018). Production of cellulose nanoparticles from blue agave waste treated with environmentally friendly processes. *Carbohydrate Polymers*, *183:* 294-302.

Rocha, George & Silva, Vinícius & Martín Medina, Carlos & Goncalves, Adilson Roberto & Nascimento, Viviane & Souto-Maior, Ana. (2013). Effect of Xylan and Lignin Removal by Hydrothermal Pretreatment on Enzymatic Conversion of Sugarcane Bagasse Cellulose for Second Generation Ethanol Production. *Sugar Technology*. 10.1007/s12355-013-0218-9.

Rolly S., Gonzales R., Periyasamy & Kim SH. (2016). Effect of severity on dilute acid pretreatment of lignocellulosic biomass and the following hydrogen fermentation. *International Journal of Hydrogen Energy*.

Sadhukhan J., Martínez- Hernández E., Murphy R., Ng D., Hassim M., Siew K., Yoke W., Jaye I., Leung M., Hang P., & Andiappan V. (2018). Role of bioenergy, biorefinery and bioeconomy in sustainable development: Strategic pathways for Malaysia. *Renewable and Sustainable Energy Reviews, 81*: 1966-1987.

Sambusiti, Cecilia & Ficara, Elena & Malpei, Francesca & Steyer, J-P & Carrere, Hélène. (2013). Effect of sodium hydroxide pretreatment on physical, chemical characteristics and methane production of five varieties of sorghum. *Energy, 55:*449–456.

Sanchez, A., Sanchez, S., Dueñas, P. *et al.* (2020). The Role of Sustainability Analysis in the Revalorization of Tequila Residues and Wastes Using Biorefineries. *Waste Biomass Valor 11:* 701–713

Santos, V., Ely, R., Szklo, A., Magrini, A. (2016). Chemicals, electricity and fuels from bio refineries processing Brazil's sugarcane bagasse: Production recipes and minimum selling prices. *Renewable and Sustainable Energy Reviews 53:* 1443-1458

Savou V., Grause G., Kumagai S., Saito Y., Kameda T. & Yoshioka T. (2019). Pyrolysis of sugarcane bagasse pretreated with sulfuric acid. *Journal of the Energy Institute, 92:*1149-1157.

Savou, V., Kumagai, S., Saito, Y. *et al.* (2019) Effects of Acetic Acid Pretreatment and Pyrolysis Temperatures on Product Recovery from Fijian Sugarcane Bagasse. *Waste Biomass Valor.*

Senthivelan T., Kanagaraj J., Panda R., Narayani T. (2019). Screening and production of a potential extracellular fungal laccase from Penicillium chrysogenum: Media optimization by response surface methodology (RSM) and central composite rotatable design (CCRD). *Biotechnology Reports*, 23.

Shah T., Ali S., Afzal A., & Tabassum R. (2018). Effect of Alkali Pretreatment on Lignocellulosic Waste Biomass for Biogas Production. *International journal of Renewable Energy Research 8: 1318-1326*

Shah, T. A. (2018).Effect of Alkalis pretreatment on Lignocellulosic Waste Biomass for Biogas Production. *International Journal of Renewable Energy Research 8(3):* 1318-1326.

Shell BV (2011). Shell Energy Scenarios to 2050

Shimizu, S., Yokoyama, T., Akiyama, T., Matsumoto, Y., (2012). Reactivity of lignin with different composition of aromatic syringyl/guaiacyl structures and erythro/threo side chain structures in b-o-4 type during alkaline delignification: As a basis for the different degradability of hardwood and softwood lignin. *Journal of Agricultural and Food Chemistry. 60 (26)*: 6471–6476.

Simanungkalit, S. P., Mansur, D., Nurhakim, B., Agustin, A., Rinaldi, N., Fitriady, M. A., Nurhakim, B. (2017). Hydrothermal pretreatment of palm oil empty fruit bunch Hydrothermal Pretreatment of Palm Oil Empty Fruit Bunch. *AIP Conference Proceedings.* https://doi.org/10.1063/1.4973138

Song, H., Clarke W.P. & Blackall, L.L (2005) Concurrent Microscopic Observations an Activity Measurements of Cellulose Hydrolyzing and Methanogenic Populations during the Batch Anaerobic Digestion of Crystalline Cellulose. *Biotechnology and Bioengineering*, *91:* 369–378.

Sun S., Sun S., Cao X., Sun R. (2016). The role of pretreatment in improving the enzymatic hydrolysis of lignocellulosic materials. *Bioresource Technology 199:* 49-58.

Sun, X.F., Xu, F., Sun, R.C., Wang, Y.X., Fowler, P., & Baird M.S. (2004). Characteristics Of Degraded Lignins Obtained From Steam Exploded Wheat Straw. *Polymer Degradation and Stability. 86:245–256.*

Taherzadeh M.J. & Karimi K. (2007) Acid-Based Hydrolysis Processes for Ethanol from Lignocellulosic Materials: A Review. *Bioresources. 2:*472-99.

Thomsen, Sune & Spliid, Henrik & Østergård, Hanne. (2014). Statistical prediction of biomethane potentials based on the composition of lignocellulosic biomass. *Bioresource Technology*. *154:*80–86. 10.1016/j.biortech. 12.029.

Tsapekos P., Kougias P. Angelidaki I. (2018). Mechanical pretreatment for increased biogas production from lignocellulosic biomass; predicting the methane yield from structural plant components. *Waste Management*, *78:* 903-910

Ullah K., Sharma K., Dhingra S., Braccio G., Ahmad M., & Sofia S. (2015). Assessing the lignocellulosic biomass resources potential in developing countries: A critical review. *Renewable and Sustainable Energy Reviews*, *51:* 682-698.

Velázquez, B., Meneses, O., Gaibor, J., Niño, Z. (2018). Review of Mathematical Models for the Anaerobic Digestion Process. DOI:10.5772/intechopen.80815. Retrieved from https://www.intechopen.com/books/anaerobic-digestion/review-of-mathematical-models-for-the-anaerobic-digestion-process

Vieira S., Vetroni M., Novak A., Moro C., de Francisco C., Porto L., Bittencourt E. (2020). Sustainability of sugarcane lignocellulosic biomass pretreatment for the production of bioethanol. *Bioresource Technology*.

Wang, Y., Joshee, N., Cao, W. *et al.* (2019). Continuous hydrogen production by dark and photo co-fermentation using a tubular multi-cycle bio-reactor with Paulownia biomass. *Cellulose*, *26:* 8429–8438.

Wang, Zhixun & Sun, Shitong & Lin, Xiongjie & Liu, Chang & Tong, Ning & Sui, Quan & Li, Zhengtian. (2019). A remote integrated energy system based on cogeneration of a concentrating solar power plant and buildings with phase change materials. *Energy Conversion and Management*, *187:* 472-485. 10.1016/j.enconman.2019.02.094.

Williams L., Emerson R., & Shankar T. (2017). Biomass Compositional Analysis for Conversion to Renewable Fuels and Chemicals. *Intechopen*. Retrieved from https://www.intechopen.com/books/biomass-volume-estimation-and-valorization-for-energy/biomass-compositional-analysis-for-conversion-to-renewable-fuels-and-chemicals

Williams, C. Luke, Westover, Tyler L., Emerson, Rachel M., Tumuluru, Jaya Shankar, & Li, Chenlin. (2015). Sources of biomass feedstock variability and the potential impact on biofuels production. *Bioenergy Resources 9:*1-14. doi:10.1007/s12155-015-9694-y.

Woo A., Conag A., Igdon R., Toledo A., & Malila J. (2019). Potentials of agricultural and agro-industrial crop residues for the displacement of fossil fuels: A Philippine context. *Energy Strategy Reviews*, *23:* 100-113.

Xiao, Chao & Liao, Qiang & Fu, Qian & Huang, Yun & Chen, Hao & Zhang, Hong & Xia, Ao & Zhu, Xun & Reungsang, Alissara & Liu, Zhidan. (2019). A solar-driven continuous hydrothermal pretreatment system for biomethane production from microalgae biomass. *Applied Energy*, *236:* 1011-1018.

Zahan, K. A. & Kano M. (2018). Biodiesel Production from Palm Oil, Its By-Products, and Mill Effluent: A Review. *Energies 1–25*.

Zianor Z., Beg M., Rosli M., Ramli R., Junadi N., Moshiul A. (2017). Spherical nanocrystalline cellulose (NCC) from oil palm empty fruit bunch pulp via ultrasound assisted hydrolysis. *Carbohydrate Polymers*, *162:* 115-120

Appendix 1: Pareto charts interactions operational conditions with response variables.

Sugarcane bagasse

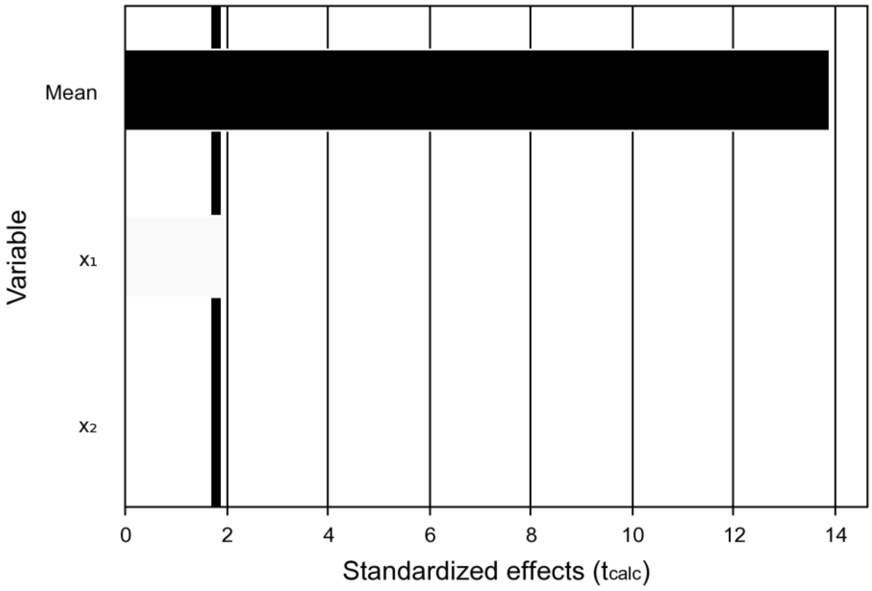

Figure 27 Pareto Chart showing the individual and coupled interactions between CCRD independent variables and glucose release from alkaline hydrothermally pretreated sugarcane bagasse (SCB). x1:Temperature (°C); x2:NaOH concentration (M) ; x3: Retention time (min

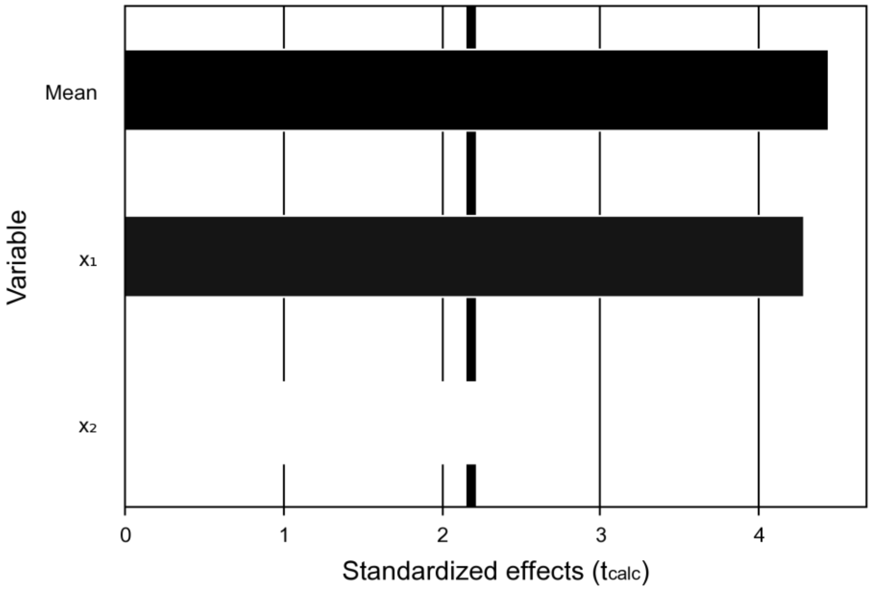

Figure 28 Pareto Chart showing the individual and coupled interactions between CCRD independent variables and arabinose release from alkaline hydrothermally pretreated sugarcane bagasse (SCB). x1:Temperature (°C); x2:NaOH concentration (M) ; x3: Retention time (m

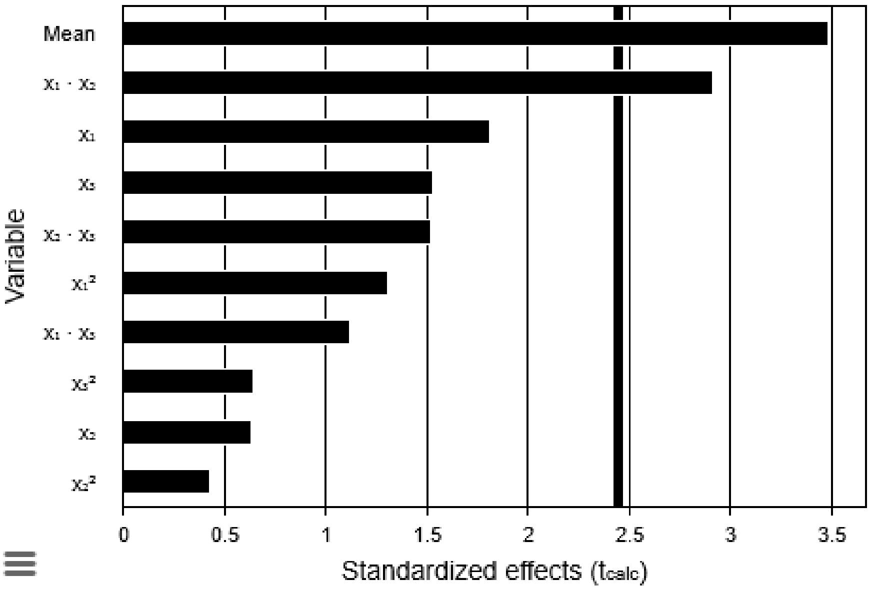

Figure 29 Pareto Chart showing the individual and coupled interactions between CCRD independent variables and delignification of sugarcane bagasse (SCB) by alkaline hydrothermally pretreatment. x_1:Temperature (°C); x_2:NaOH concentration (M) ; x_3: Retention time (min)

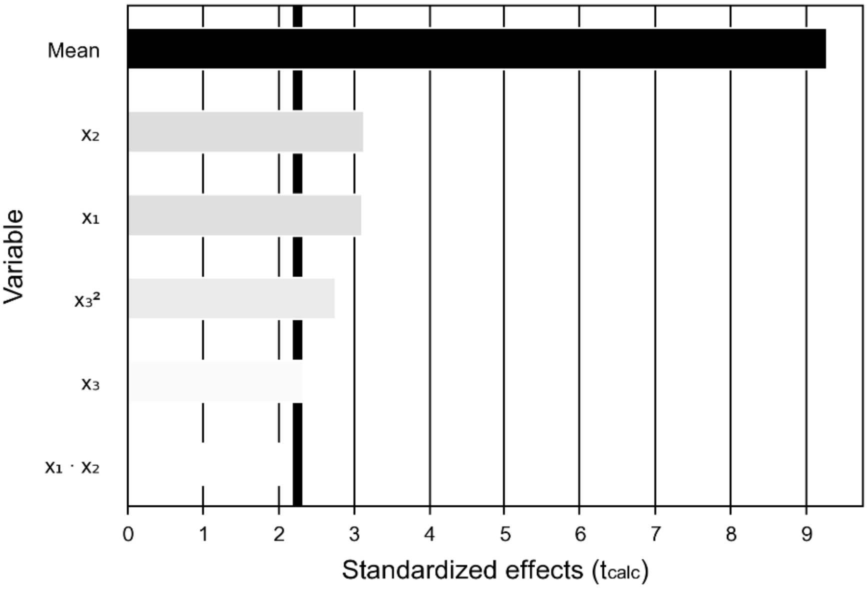

Figure 30 Pareto Chart showing the individual and coupled interactions between CCRD independent variables and solids recovery from alkaline hydrothermally pretreated sugarcane bagasse (SCB). x1:Temperature (°C); x2:NaOH concentration (M) ; x3: Retention time (min

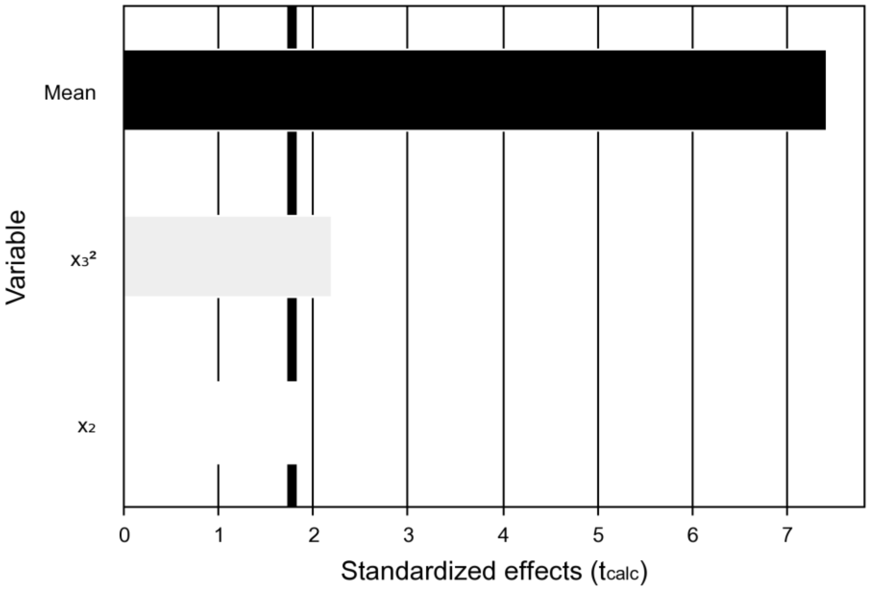

Figure 31 Pareto Chart showing the individual and coupled interactions between CCRD independent variables and biomethane potential (BMP) from alkaline hydrothermally pretreated sugarcane bagasse (SCB) x_2:NaOH concentration (M) ; x_3: Retention time (min)

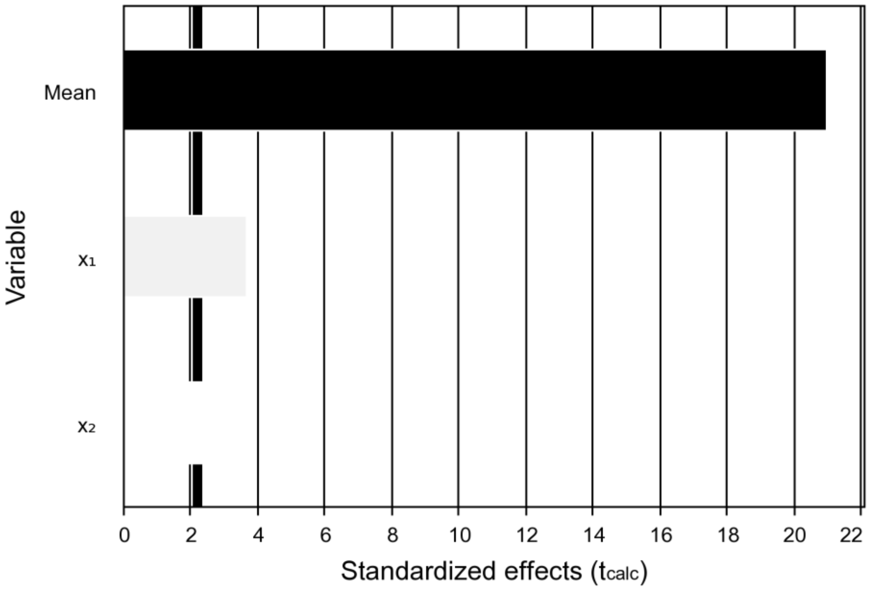

Figure 32 Pareto Chart showing the individual and coupled interactions between CCRD independent variables and methane composition of alkaline hydrothermally pretreated sugarcane bagasse (SCB) hydrolysates. x_1:Temperature (°C); x_2:NaOH concentration (M) ; x_3: Retention time (min)

Empty fruit bunch

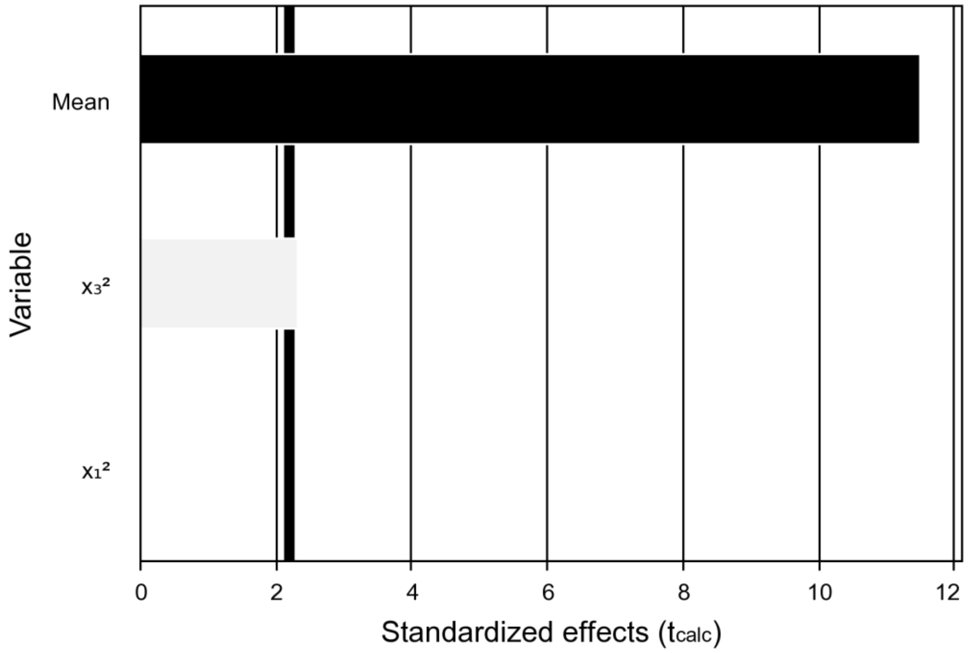

Figure 33 Pareto Chart showing the individual and coupled interactions between CCRD independent variables and glucose release from alkaline hydrothermally pretreated empty fruit bunch (EFB). x1:Temperature (°C); x2:NaOH concentration (M) ; x3: Retention time (min

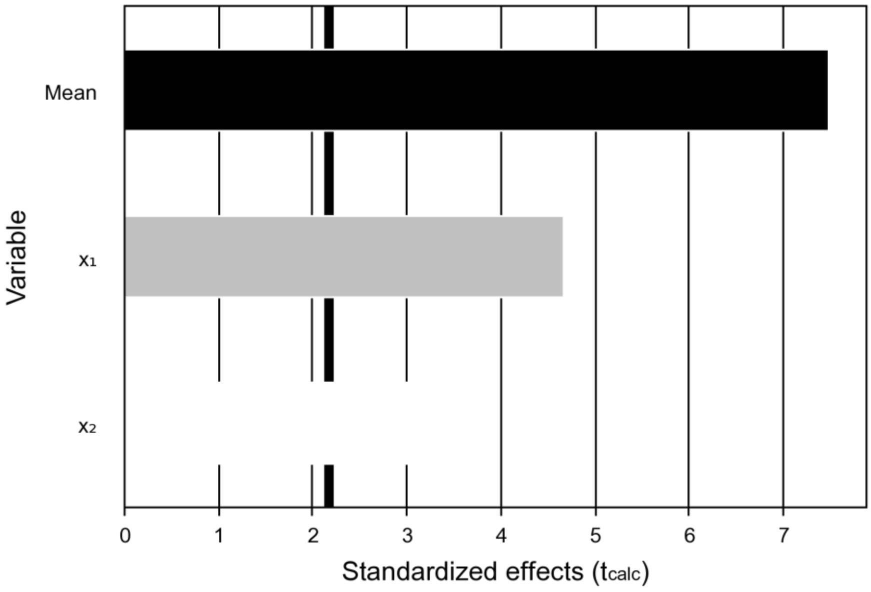

Figure 34 Pareto Chart showing the individual and coupled interactions between CCRD independent variables and arabinose release from alkaline hydrothermally pretreated empty fruit bunch (EFB). x1:Temperature (°C); x2:NaOH concentration (M) ; x3: Retention time (m

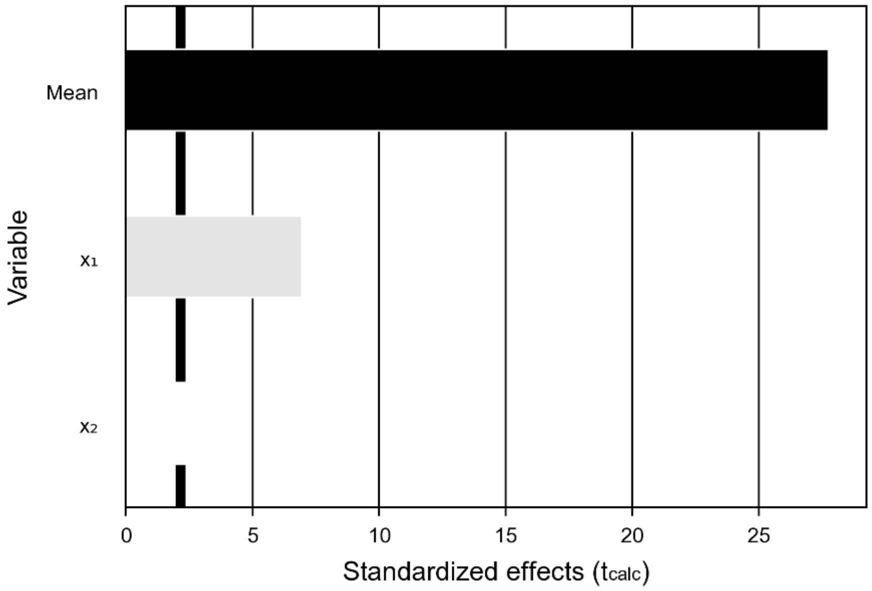

Figure 35 Pareto Chart showing the individual and coupled interactions between CCRD independent variables on solids recovery from alkaline hydrothermally pretreated empty fruit bunch (EFB). x1:Temperature (°C); x2:NaOH concentration (M)

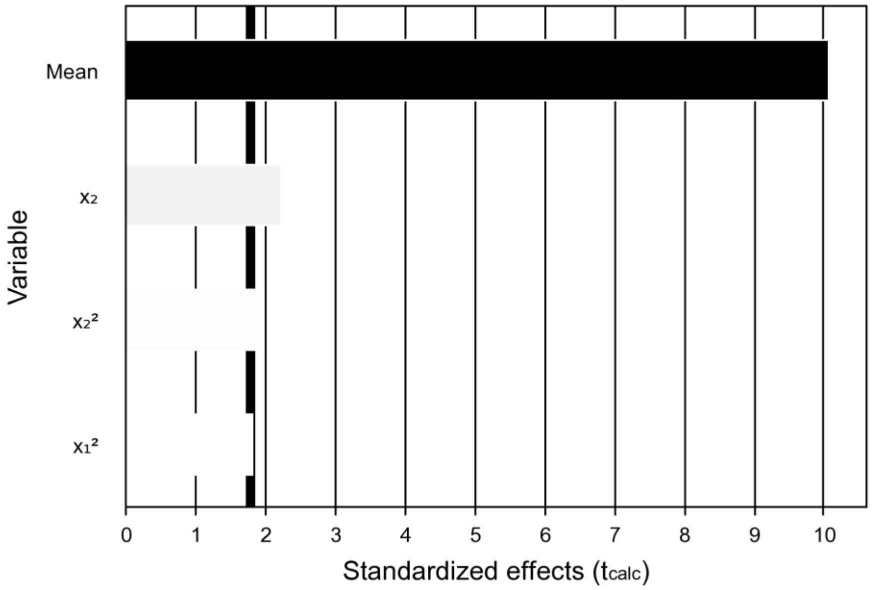

Figure 36 Pareto Chart showing the individual and coupled interactions between CCRD independent variables on biomethane potential (BMP) from co digestion of empty fruit bunch (EFB) hydrolysates x1:Temperature (°C); x2:NaOH concentration (M)

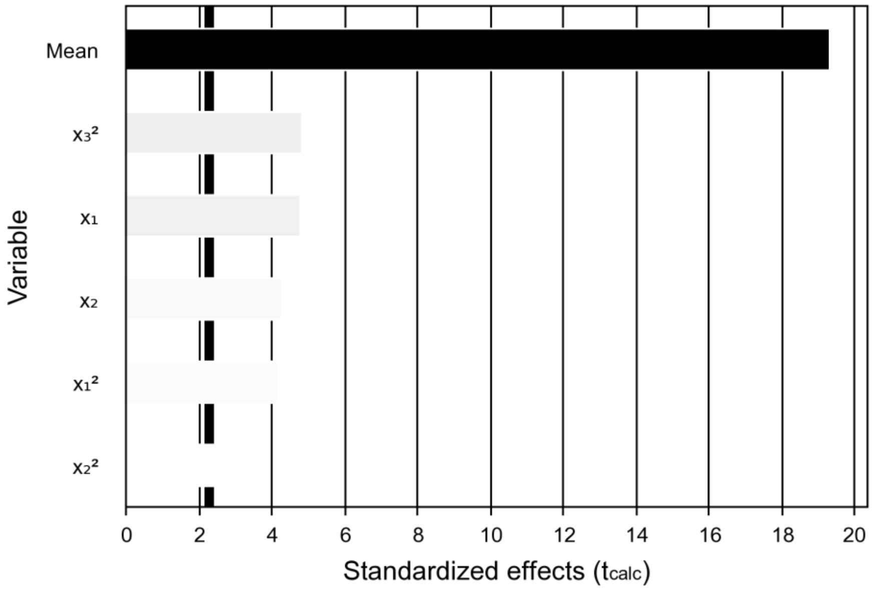

Figure 37 Pareto Chart showing the individual and coupled interactions between CCRD independent variables and methane composition of alkaline hydrothermally pretreated empty fruit bunch (EFB) hydrolysates. x_1:Temperature (°C); x_2:NaOH concentration (M) ; x_3: Retention time (min)

Agave bagasse

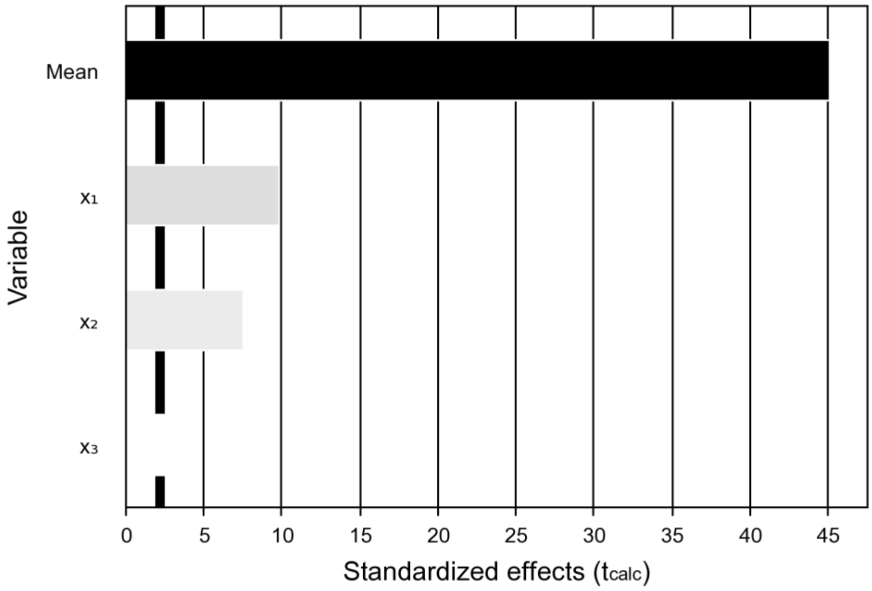

Figure 38 Pareto Chart showing the individual and coupled interactions between CCRD independent variables and glucose release from alkaline hydrothermally pretreated agave bagasse (AB). x_1:Temperature (°C); x_2:NaOH concentration (M) ; x_3: Retention time (min)

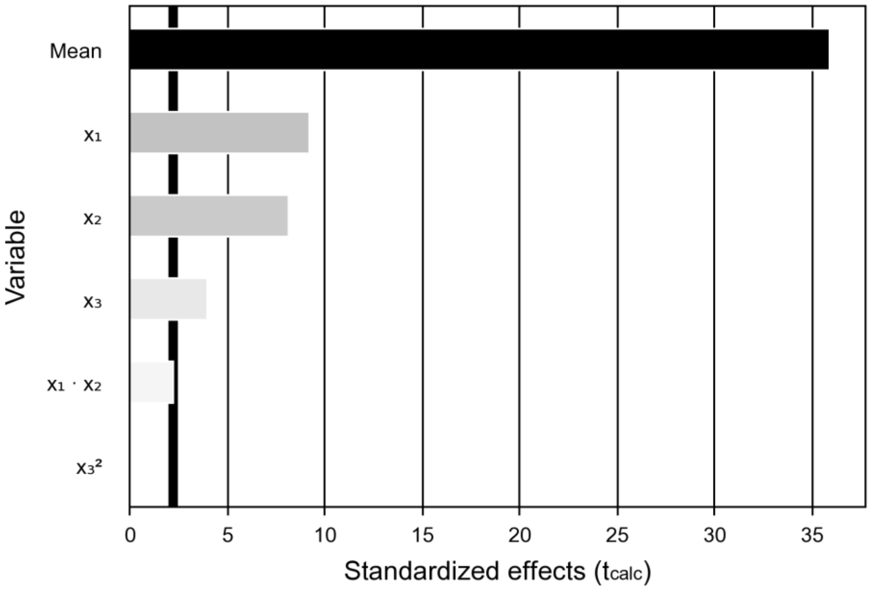

Figure 39 Pareto Chart showing the individual and coupled interactions between CCRD independent variables and arabinose release from alkaline hydrothermally pretreated agave bagasse (AB). x_1:Temperature (°C); x_2:NaOH concentration (M) ; x_3: Retention time (min)

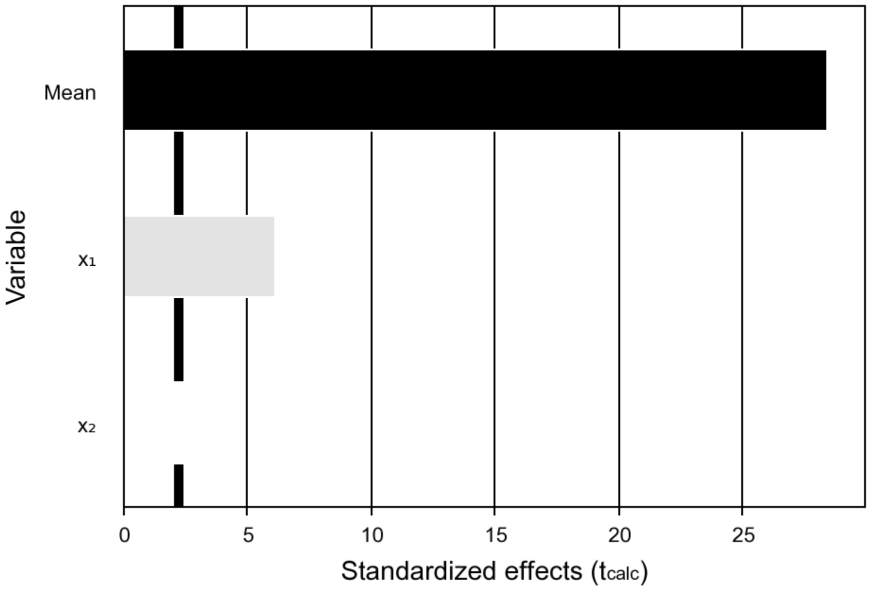

Figure 40 Pareto Chart showing the individual and coupled interactions between CCRD independent variables on solids recovery from alkaline hydrothermally pretreated agave bagasse (AB) x1:Temperature (°C); x2:NaOH concentration (M)